

## ***Chapter 19***

# ***The Physics of Electrosensory Worlds***

Jan Benda

[jan.benda@uni-tuebingen.de](mailto:jan.benda@uni-tuebingen.de)

Neuroethology, Institute for Neurobiology, Eberhard Karls Universität, Tübingen, Germany

### ***Synopsis***

The electric sense of electric fish is an alien sense to us for which we have no intuition. Starting with Hans Lissmann's early studies in the 1950s, step-by-step we have gained more insights into the electric world, based on behavioral experiments, simulations and the physics of electrostatics. This chapter reviews and extends fundamental aspects of electrolocation, electronavigation and electrocommunication and points out quantitative relations that need to be taken into account in future studies on the sensory ecology of these fascinating fishes.

### ***Abstract***

Electric fish generate electric fields to infer properties of their environment and to communicate with each other. What does an electrosensory world look like? What are the basic physical laws governing electric image formation? This is discussed in four sections: temporal and spatial properties of electric fields generated by electric fish, electrolocation of small objects, electronavigation based on large nonconducting boundaries, and electrocommunication by frequency modulations of beats. Guided by the specific physics of these problems, behavioral, physical, and simulation findings are set into context. The dipole nature of the fish's electric field and of polarized nearby objects inevitably limit electrolocation to the fish's near field. Detection of capacitive objects as a different electric color is only possible if capacity, water conductivity and spectral properties of the fish's electric field match. Water surface and large rocks as large nonconducting boundaries provide cues which are potentially detectable within a range of a meter and usable for electronavigation. Electrocommunication signals cover ranges up to 2 m and in wave fish are frequency modulations of beats on various timescales, ranging from tens of milliseconds to several minutes. We are just starting to understand their variety, their meaning and behavioral significance in courtship, breeding, aggression, group cohesion, etc. In addition to physical constraints, many selection pressures from predators and conspecifics act on electrosensory systems. We need more field data and need to explore the electric properties of ecological niches occupied by electric fish to really understand their adaptations and the costs of the various selection pressures.

## 19.1 Introduction

In addition to the visual sense, fish and some amphibians have developed the lateral line as a far sense for detecting prey and conspecifics, and for navigating without visual cues at night, in murky or turbid waters, or in great depths (Bleckmann and Zelik, 2009). Many fish have developed yet another far sense, the passive electrosensory system. In most non-teleost fishes, like rays, sharks, sturgeons, paddlefish, it is based on Lorenzinian Ampullae. Only a few teleost fishes developed various types of ampullary organs: Xenomystinae and Gymnarchidae (African knifefish), Mormyridae (African elephantfish), Siluriformes (catfish), and Gymnotiformes (Neotropical knifefish) (Bullock, Bodznick, and Northcutt, 1983). The ampullary system detects low frequency ( $< 50$  Hz) electric fields with high sensitivity (below  $1\ \mu\text{V}$  down to  $10\ \text{nV}$  in marine rays and sharks, Kalmijn, 1974). Some fish, namely the Gymnarchidae, Mormyridae, and Gymnotiformes electric fish, went further and developed electric organs that actively generate electric fields. Combined with specialized electroreceptors that measure modulations of the self-generated electric fields, this forms an active electrosensory system. Electric fish exclusively inhabit tropical aquatic habitats with low water conductivities (Crampton and Albert, 2006).

How does the electrosensory world of electric fish look like? For what purpose is it used? What are the physical constraints? What exactly is the fitness advantage the electrosensory sense provides in comparison to “normal fish”? A text-book myth is that electrosensory systems allow fish to forage in murky waters and during night-times where the visual system fails. This is most certainly wrong. If you have ever looked into a tropical stream at night, or at an Amazonian fish market, then you know that many non-electric fish successfully survive and reproduce quite well in these conditions, probably because of their sophisticated lateral line sense. For an understanding of the subtle and specific advantages an electrosensory system provides, we need to look closer.

The physics of quasistationary electrodynamics is key for understanding the principles of electrosensory stimuli. In contrast to visual or auditory systems, electric fish do not emit propagating waves. Electric fields spread with the speed of light, that is nearly instantaneously within the relevant range of a few meters. In contrast to echolocation of bats this precludes the use of conduction delays for localization, but comes with the advantage of preserving fine temporal features, like the submillisecond waveform features of pulse fish (Hopkins, 1999). The physics of electrostatics was instrumental for early works on electrosensory systems (Lissmann and Machin, 1958; Knudsen, 1975; Heiligenberg, 1975; Bacher, 1983) and more recent theoretical work still provides inspiring insights (Rasnow and Bower, 1996; Sicardi, Caputi, and Budelli, 2000). Whereas many thoughtful behavioral, physical, and neurophysiological experiments and realistic simulations provide us with a lot of details, theoretical insights based on highly abstracted and simplified models provide us with quantitative and functional relations and highlight interdependencies at the core of an electrosensory world. These theoretical results are needed to formulate precise questions that then allow us to quantitatively assess the relevant parameter of the sensory ecology of the electric sense.

First, basic temporal and spatial properties of the dipolar electric fields generated by electric fish are introduced. The section on electrolocation reviews the physics of how small objects distort the fish’s electric field and produce electric images. The effects of large nonconducting boundaries, like the water surface or a big rock, that are governed by a much more favorable physics than the one of small objects, have been largely neglected so far. This is discussed in the section on electronavigation. The last section touches on various types of electrocommunication signals produced by electric fish, with a focus on gymnotiform wave-type fish. The chapter is concluded with a vision on future research on the electric world of electric fishes in their natural microhabitats.

## 19.2 Electric organ discharge

The defining feature of active electrosensation is the generation of a bioelectric field. Electric fish developed electric organs of neurogenic (in Aptereronotidae, Kirschbaum, 1983) or myogenic origin in their tails (Bennett, 1970). Large electrocytes are stacked in rows and are discharged more or less synchronously. The action potentials generated by each electrocyte sum up to result in a compound action potential large enough to be detectable as an external electric field. The generated electric field resembles that of a dipole (Fig. 19.1 A). Typically, during the main discharge the

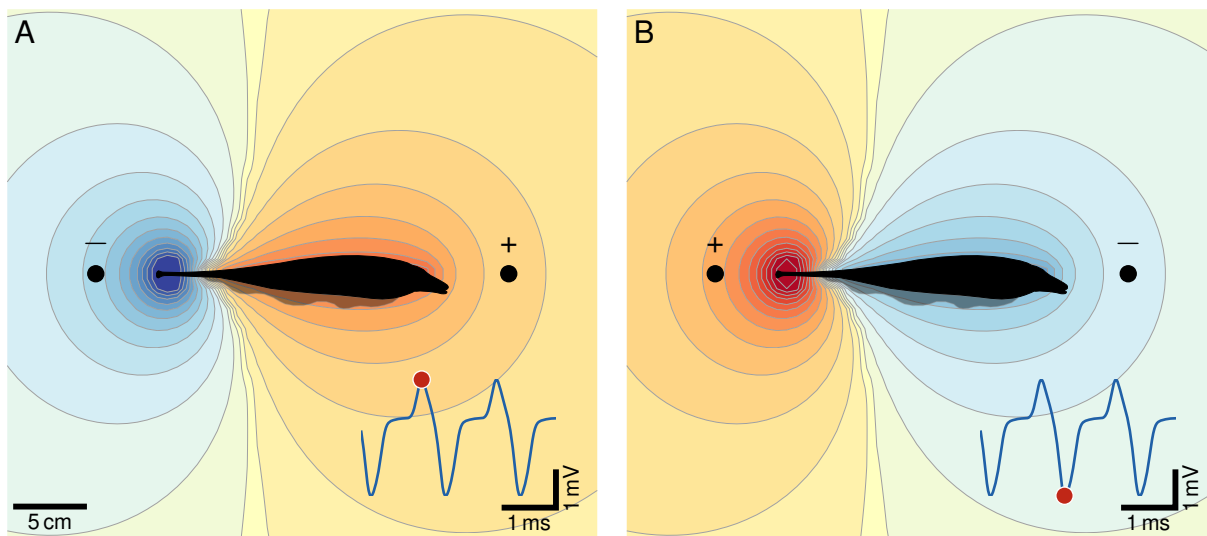


**Figure 19.1:** Electric organ discharges. **A** The electric organ discharge (EOD) generates a dipolar electric field around the fish. During the positive phase of the EOD waveform (red dot in inset) the field potential is positive around the head (isopotential lines in red) and negative around the tail (blue colors). **B** The polarity of the electric field switches during the negative phase of the EOD waveform. The EOD waveform shown in the insets is a head to tail recording of an *Apteronotus rostratus* with the two electrodes placed at the head and at the tail, respectively (filled circles).

head region is polarized positively and the tail negatively. The polarity is reversed at negative phases of the electric organ discharges (EOD, Fig. 19.1 B).

### 19.2.1 EOD waveform

The EOD waveform can be readily measured by recording the voltage between two electrodes placed in the vicinity of the fish. In a head-to-tail recording, one electrode is located near the head and the other one near the tail (Fig. 19.1). This results in a maximal signal amplitude in a standardized electrode configuration. Particularly in Gymnotiformes with their elongated electric organs, electrocytes are not discharged exactly at the same time (Rasnow and Bower, 1996; Rodríguez-Cattáneo<sup>1</sup>, Aguilera, Cilleruelo, Crampton, and Caputi<sup>1</sup>, 2013). Consequently the measured EOD waveform depends on electrode position (Hoshimiya, Shogen, Matsuo, and Chichibu, 1980).

#### Wave fish

Two basic types of EOD waveforms are distinguished: wave-type and pulse-type EODs. In wave-type EODs the width of each discharge is of the same order of magnitude as the interval from one discharge to the next. Wave-type EODs are continuous and periodic and often resemble a sine wave (Fig. 19.2 A–C). When played on a loudspeaker, wave type fish simply sound like tones of constant pitch. Many species of the neotropical Gymnotiform fishes generate wave-type EODs, whereas *Gymnarchus niloticus* is the only species in Africa with a wave-type EOD (Lissmann, 1951). The amplitude of wave-type EODs is small, typically in the range of a few or tens of millivolts.

Wave type fish are characterized by EOD frequency (number of discharges per second) that stays remarkably constant (Moortgat, Keller, Bullock, and Sejnowski, 1998), but depends on temperature (up to  $\sim 40$  Hz per Kelvin in *Apteronotus*, Lissmann, 1958; Enger and Szabo, 1968; Dunlap, Smith, and Yekta, 2000). EOD frequencies range from less than 50 Hz to more than 2 kHz. The power spectrum of a wave-type EOD is characterized by peaks at the fundamental frequency, given by the EOD frequency, and its harmonics. The relative amplitudes of the harmonics depend on EOD waveform. The more the waveform resembles a sine wave the faster the amplitudes of the harmonics drop (Fig. 19.2 AB). Vice versa, *Sternopygus* with its flat potential in between the discharges has many harmonics that easily reach into the frequency ranges of species with higher EOD frequencies (Fig. 19.2 C,

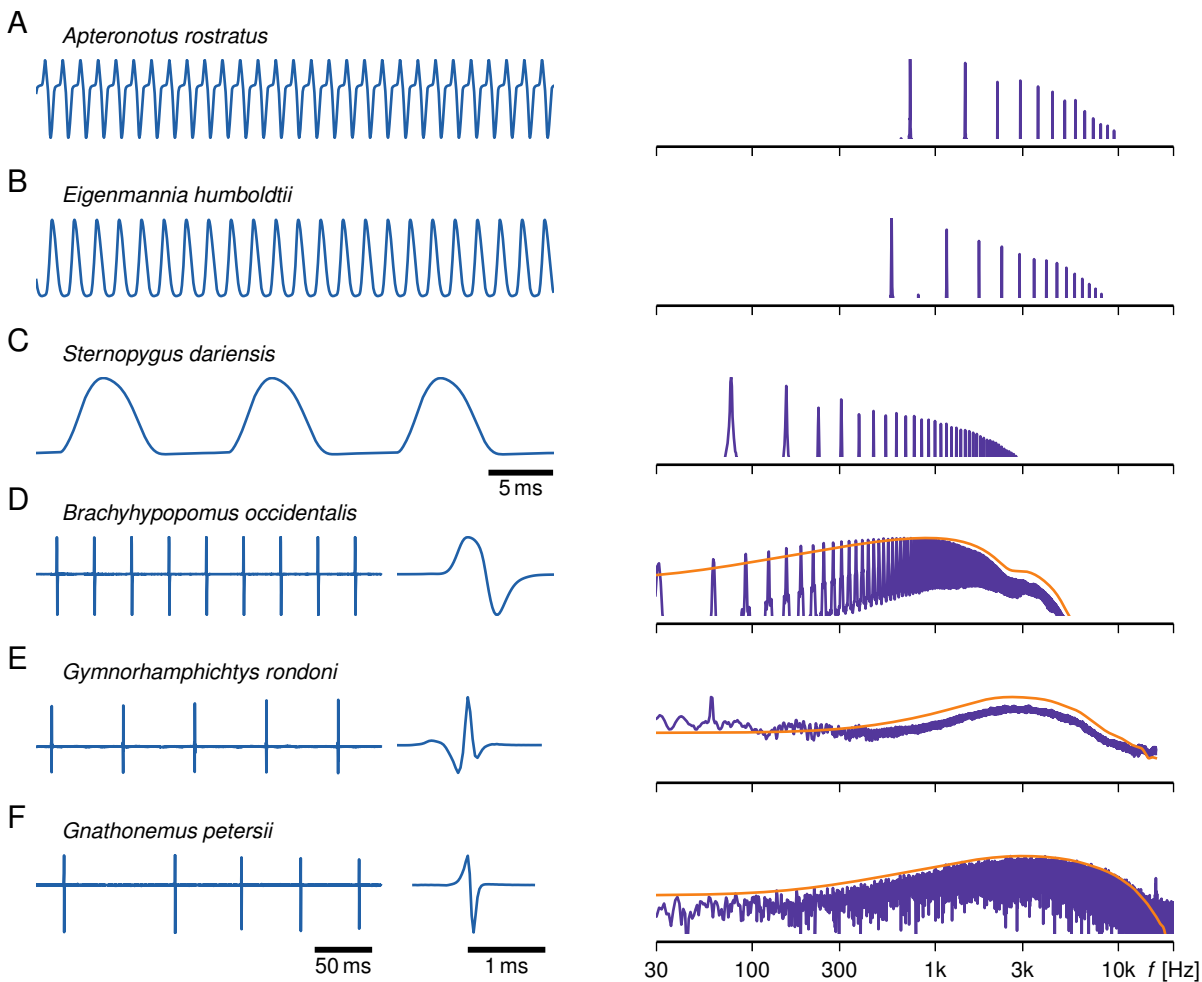


**Figure 19.2:** EOD waveforms of wave- and pulse fish. Waveforms shown in left column, corresponding logarithmic power spectra in right column. **A – C** EODs of wave fish are continuous and periodic waveforms where each single EOD occupies a significant fraction of the period. **A** *Aptereronotus rostratus* with an EOD frequency (EOD $f$ ) of 728 Hz. The power spectrum has peaks at integer multiples of the fundamental at EOD $f$ . The relative peak amplitudes depend on the shape of the EOD waveform. **B** *Eigenmannia humboldtii* with EOD $f$  = 577 Hz. **C** *Sternopygus dariensis* with EOD $f$  = 77 Hz. **D – F** Waveforms of pulse fish are brief pulses with one or more positive and negative peaks that are spaced by much longer intervals. **D** In Gymnotiform pulse-type electric fish the pulses are generated periodically. Here, a recording of *Brachyhypopomus occidentalis* with EOD $f$  = 31 Hz is shown. The power spectrum of the recording (blue) has peaks at integer multiples of the EOD frequency, their amplitude is approximately given by the power spectrum of a single pulse (orange). **E** The Gymnotiform pulse fish *Gymnorhamphichtys rondoni* has a narrower and more complex waveform. In the recording it is discharging at 16 Hz. **F** Mormyridae, like *Gnathonemus petersii* shown here, are pulse-type fish that discharge irregularly. There are no harmonic peaks in the power spectrum of the recording, but again the amplitude is given by the single pulse power spectrum.

Henninger, Krahe, Sinz, and Benda, 2020).

Each species covers a specific range of EOD frequencies, often close to a full octave (Hopkins, 1974a; Hopkins and Heiligenberg, 1978; Kramer, Kirschbaum, and Markl, 1981; Crampton and Albert, 2006). Whereas low frequency fish like *Sternopygus* or *Eigenmannia* nicely separate in EOD frequencies below 600 Hz (Hopkins, 1974b; Hopkins and Heiligenberg, 1978; Stamper, Carrera-G, Tan et al., 2010; Henninger, Krahe, Sinz, and Benda, 2020), EOD frequencies above 600 Hz are often occupied by several species (Bullock, 1969; Steinbach, 1970; Hopkins, 1974a; Kramer, Kirschbaum, and Markl, 1981). Within each species individuals usually have different EOD frequencies. EOD frequency can be sexually dimorphic. In non-Aptereronotidae, like *Eigenmannia* sp. or *Sternopygus* sp., females tend to have higher EOD frequencies than males (Hopkins, 1972, 1974a) and *Sternopygus macru-*

*rus* males prefer the higher female EOD frequencies (Hopkins, 1972). *Apteronotus albifrons* follows this pattern (Dunlap, Thomas, and Zakon, 1998), but *Apteronotus leptorhynchus* has a strong dimorphism with males having higher EOD frequencies than females (Meyer, Leong, and Keller, 1987). Other Apteronotidae do not seem to have a sexual dimorphism in EOD frequency (Smith, 2013).

Whether gymnotiform fish are able to discriminate EOD waveforms is not yet understood. Whereas Kramer (1999) was able to demonstrate that *Eigenmannia* is able to differentiate female from male EOD waveforms that overlap in frequencies (Hopkins, 1974a) and Dunlap and Larkins-Ford (2003) have shown that *Apteronotus leptorhynchus* chirp more to a real fish than to a sinewave mimic, Fugère and Krahe (2010) failed to elicit differences in chirp responses to playback of EOD waveforms from various species.

### **Pulse fish**

Pulse-type EODs are much more narrow than the intervals between pulses (Fig. 19.2 D–F). Also, on an absolute scale, most of them are clearly shorter than 1 ms. The shorter the pulses the higher the peak frequencies of single pulse power spectra (Hopkins and Westby, 1986). Pulse-type EODs are usually larger in amplitude than wave-type EODs, reaching amplitudes of up to a few volts, or, in case of electric eels, up to 800 V (de Santana, Crampton, Dillman et al., 2019). All Mormyridae produce pulse-type EOD waveforms (Fig. 19.2 F). Gymnotiform pulse-type electric fish generate pulses periodically with some preferred frequency (below approximately 150 Hz) that, like in wave fish, increases with water temperature (Coates, 1954; Silva, Quintana, Galeano, Errandonea, and Macadar, 1999). Consequently, the power spectrum has peaks at integer multiple of the EOD frequency, which in comparison to wave fish are wider, because the discharge frequency is not that stable (Fig. 19.2 D). The amplitude of the peaks is approximately given by the single pulse spectrum, because the power spectrum is a convolution of the single pulse spectrum with the Dirac-comb spectrum of the periodic discharge. In contrast, Mormyridae and electric eels time their EODs irregularly depending on their needs for electrolocation. This results in smeared out power spectra that reflect just the single pulse spectrum (Fig. 19.2 F). In both Gymnotiformes and Mormyridae, and in contrast to wave-type fish, EOD frequency depends on movement activity. Right before Gymnotiform pulse fish get active, they raise their EOD frequency (Lissmann and Schwassmann, 1965; Jun, Longtin, and Maler, 2014). Made audible by means of a loud speaker, higher frequency pulse fish generate a rattling sound with a pitch that occasionally is increased, in particular when getting closer with an electrode. In lower frequency pulse fish, the single pulses can be easily perceived as separated clicks.

EOD waveforms in pulse fish are very diverse (Hopkins and Heiligenberg, 1978; Kramer, Kirschbaum, and Markl, 1981; Hopkins and Bass, 1981). They differ in duration and in their temporal fine structure, i.e. in the number, sequences and relative amplitudes of peaks within each EOD (Fig. 19.2 D–F). EOD waveforms are species specific (Crampton and Albert, 2006; Arnegard, McIntyre, Harmon et al., 2010) and are a major cue for reproductive isolation (Feulner, Plath, Engelmann, Kirschbaum, and Tiedemann, 2009). Pulse fish EODs often show a sexual dimorphism with male EODs being longer than female EODs (Hopkins, 1999). EOD waveforms differ even between individuals of the same species (Friedman and Hopkins, 1996; Machnik and Kramer, 2008) and the fish are able to discriminate these (Hopkins and Bass, 1981; Graff and Kramer, 1992) based on temporal cues (Heiligenberg and Altes, 1978). EOD waveform also depends on environmental factors like temperature (Harder, Schief, and Uhlemann, 1964; Silva, Quintana, Galeano, Errandonea, and Macadar, 1999) and conductivity (Caputi, Silva, and Macadar, 1998) and both pulse amplitude and discharge frequency are subject to circadian and seasonal plasticity (Harder, Schief, and Uhlemann, 1964; Franchina and Stoddard, 1998; Silva, Perrone, and Macadar, 2007).

Unbalanced pulse waveforms may contain a DC component that can be detected by passively electroreceptive predators or other electric fish. Consequently, there is a selection pressure towards shorter and more balanced EOD waveforms (Stoddard, 1999; Stoddard and Markham, 2008; Stoddard, Tran, and Krahe, 2019). Sexual selection for longer and unbalanced EOD waveforms in males seems to counteract this (Machnik and Kramer, 2008). As another selection pressure for shorter EOD waveforms, reduction in temporal overlap of EODs in social pulse fish has been suggested (Hopkins, 1980).



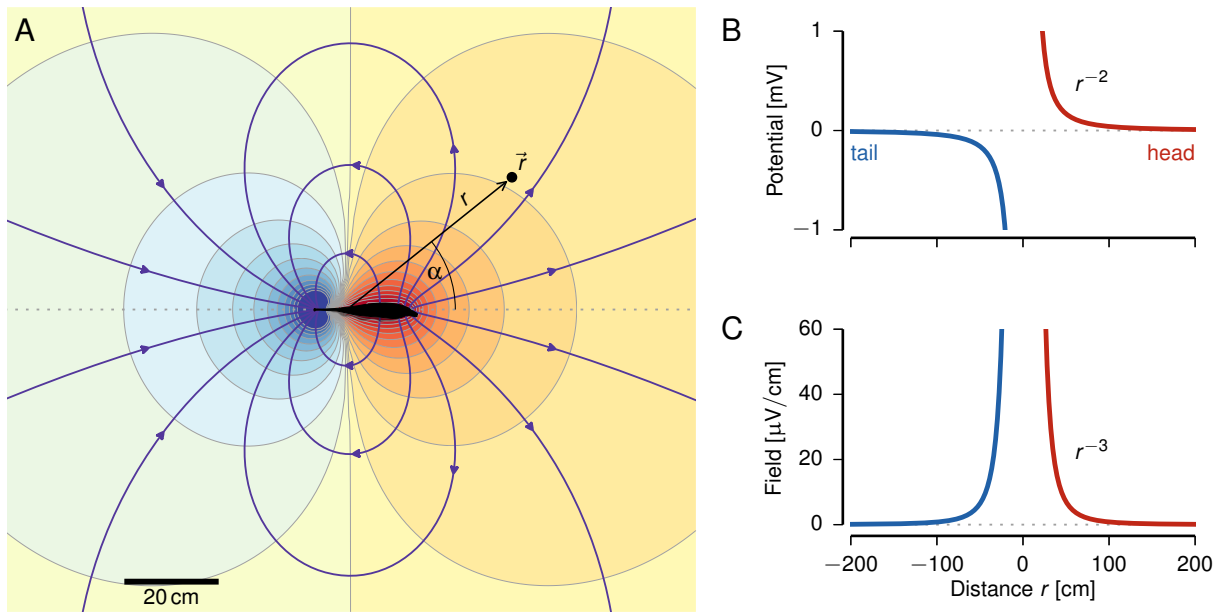


**Figure 19.3:** Electric far field. **A** The electric far field of any electric fish is that of a dipole. Isopotential lines are shown in red (positive) and blue (negative) colors, a few fieldlines (blue arrows) illustrate the corresponding electric field vectors. The field is symmetric with respect to the equatorial plane (vertical line) perpendicular to the fish's body axis. At the equatorial plane the potential is zero. The field is symmetric with respect to rotation around the body axis. At points  $\vec{r}$  at a given distance  $r$  and direction  $\alpha$  from the body axis the potential of the field is the same. **B** The potential of a dipole field drops with distance squared. Shown is the potential along the body axis (dotted line in A). The polarities of the head and tail region of the field are of opposite signs. **C** The electric field strength is the negative spatial derivative of the electric potential. The electric field strength is the relevant quantity that is transmitted by electroreceptors. It drops with distance cubed.

### 19.2.2 Electric field geometry

Let us have a closer look at the spatial properties of the electric field generated by electric fish in an infinite homogeneous water volume with no objects in it. In the far field, i.e. at distances larger than the size of the fish, the spatial geometry of the electric field approaches that of an ideal dipole (Knudsen, 1975; Henninger, Krahe, Sinz, and Benda, 2020). In the following we discuss the properties of the dipole field in detail and in the end contrast it with the properties of the near field, that deviates from the field of an ideal dipole.

The dipolar far field is characterized by two lobes of positive and negative potentials around the head and the tail of the fish that are perfectly symmetric to each other. The equatorial plane with zero potential is planar and perpendicular to the body axis (Fig. 19.3 A). The potential  $\phi$  of an ideal dipole field at distance  $r$  and angle  $\alpha$  from the body axis is given by<sup>1</sup>

$$\phi(r, \alpha) = \frac{I(t)s}{4\pi\sigma} \cdot \frac{\cos(\alpha)}{r^2} \quad (19.1)$$

where  $\sigma$  is the conductivity of the medium, i.e., the conductivity  $\sigma_w$  of water in case of electric fish. The magnitude of the dipole moment,  $P_I(t) = I(t)s$ , is generated by equal and opposite current sources,  $I(t)$ , that change in time according to the EOD waveform and are separated by a small distance  $s$ . Think of  $s$  as being the length of the electric organ. No matter how complicated the electric organ and the complex ways it is discharged, for purely

<sup>1</sup>The total current flowing through any sphere of radius  $r$  must equal the current  $I$  produced by a current point source at the center (charge conservation). Because of the spherical symmetry, the current densities  $\vec{J}(\vec{r})$  at any point  $\vec{r}$  on such a sphere point in radial direction,  $\vec{r}/r$ , and their magnitudes equal the source current  $I$  divided by the surface of the sphere:  $\vec{J} = I \cdot (\vec{r}/r)(4\pi r^2)^{-1}$ . According to Ohm's law, Eq. (19.5) below, current densities are directly related to the electric field  $\vec{E}$  via the conductivity  $\sigma$  of the medium. Since the electric field is the negative gradient of the electric potential, Eq. (19.3), we get by integration for the potential of a single current source the potential  $\phi_1(\vec{r}) = I(4\pi\sigma r)^{-1}$ . Adding up the potentials of two such current monopoles separated by a small distance  $s$  and of opposite polarity, and keeping only the linear term of a Taylor expansion with respect to  $s$ , results in the dipole potential Eq. (19.1).

physical reasons, its far field ( $r \gg s$ ) approaches that of an ideal dipole, Eq. (19.1). The potential of a dipole drops with distance squared (Fig. 19.3 B). It can be measured as the voltage between a measurement electrode against an infinitely far reference.

### Transdermal voltage

Electroreceptive organs measure the voltage drop,  $V_t$ , between the electric potentials at their opening on the skin of the fish,  $\phi_s$ , and at the receptor cell at the end of an epidermal plug or duct deep in the skin,  $\phi_r$ :

$$V_t = \phi_s - \phi_r \quad (19.2)$$

This is called the “transdermal potential”, or more correctly, “transdermal voltage”, because it is a difference between two potentials. It can be experimentally estimated by placing a dipole electrode close to the skin of the fish. Fotowat, Harrison, and Krahe (2013) measured transdermal voltages in freely behaving fish.

### Electric field

For the small ampullary and tuberous electroreceptor organs, the transdermal potential is well approximated by the electric field component in direction of the receptor. The electric field  $\vec{E}$  is a vector field, i.e. to each point in space  $\vec{r}$  a vector with a direction and a length, the electric field strength  $|\vec{E}|$ , is assigned. The electric field is the negative gradient, the spatial derivative, of the potential:

$$\vec{E}(\vec{r}) = -\nabla\phi(\vec{r}) = -\begin{pmatrix} \frac{\partial\phi(\vec{r})}{\partial x} \\ \frac{\partial\phi(\vec{r})}{\partial y} \\ \frac{\partial\phi(\vec{r})}{\partial z} \end{pmatrix} \quad (19.3)$$

The  $\vec{E}$  vectors of the electric field at any position  $\vec{r}$  are perpendicular to the isopotential planes where  $\phi(\vec{r}) = \text{const.}$  Within isopotential planes there is no electric field component.

According to Ohm’s law, Eq. (19.5), the electric field right in front of a receptor organ at position  $\vec{r}_r$  drives a current density  $j(\vec{r}_r) = \sigma_w \vec{E}(\vec{r}_r) \cdot \vec{n}$  into the receptor organ, which points in direction  $\vec{n}$ , usually the surface normal (McKibben, Hopkins, and Yager, 1993) with  $|\vec{n}| = 1$ . This current causes a voltage drop, the transdermal voltage, over the epidermal plug or duct of length  $d$  with conductivity  $\sigma_r$ :

$$V_t = \vec{E}(\vec{r}) \cdot \vec{n} \frac{\sigma_w}{\sigma_r} d \quad (19.4)$$

(Rasnow and Bower, 1996; Chen, House, Krahe, and Nelson, 2005). Electroreceptors respond to the projection  $\vec{E}(\vec{r}) \cdot \vec{n}$  of the electric field vector at the position of the receptor organ onto the direction the receptor is pointing to. If receptor organs point in the direction of the electric field vector, then they respond best. On the other hand, receptors oriented orthogonal to electric field vectors do not convey any information about these fields.

### Electric field lines

The electric field exerts a force on charged particles, e.g., ions, in the field, such that they move in the direction given by the electric field vector at the position of the charges. The resulting path of a particle is an electric field line (Fig. 19.3 A). Field lines connect positive with negative charges and illustrate the direction positively charged particles move. Negatively charged particles move in the opposite direction. Moving charges are electric currents, thus, electric field lines illustrate current densities  $\vec{J}$  flowing in the electric field. The electric field gives rise to current densities  $\vec{J}$ , electric current flowing through an unit area (measured in  $\text{A m}^{-2}$ ) at any point in the field. The two are related by Ohm’s law

$$\vec{J} = \sigma \vec{E} \quad (19.5)$$

where  $\sigma$  is the conductivity of the medium.

### Electric organ model

According to Thévenin's theorem, any linear network made up from voltage sources, current sources and resistances is equivalent to a single voltage source  $V_s$  and an inner resistance  $R_s$  in series. Consequently, as long as the electric organ behaves linearly we can model it by  $V_s$  and  $R_s$ , without further knowledge of the physical details of the electric organ (Fig. 19.4 A). For a given output voltage  $V_o$  of the electric organ, the current flowing through the organ is  $I = (V_s - V_o)/R_s$ . Outside the fish, the circuit is completed by a load resistance  $R_l = (c\sigma_w)^{-1}$ , which is inversely proportional to the water conductivity  $\sigma_w$ . The proportionality factor  $c$  depends on the geometry of the electric field set by tank size and static objects therein (Bell, Bradbury, and Russell, 1976). The current  $I$  generated by the electric organ needs to flow through  $R_l$  to complete the electrical circuit:  $I = V_o c \sigma_w$ . Eliminating  $V_o$  from the two equations for the current we get

$$\frac{I(t)}{\sigma_w} = \frac{cV_s(t)}{1 + c\sigma_w R_s} \quad (19.6)$$

(Heiligenberg, 1975). Plugging Eq. (19.6) into Eq. (19.1), the dipole potential reads

$$\phi(r, \alpha) = W(t) \frac{\cos(\alpha)}{r^2} \quad (19.7)$$

with the waveform factor

$$W(t) = \frac{P_V(t)}{1 + \sigma_w / \sigma_s} \quad (19.8)$$

In this equation a modified dipole moment  $P_V(t) = cV_s s (4\pi)^{-1}$  summarizes all multiplicative factors into a single parameter and the inner conductivity  $\sigma_s = (cR_s)^{-1}$  absorbs the geometry factor from the load resistance. The time dependence of  $P_V(t)$  and  $W(t)$  accounts for the temporal aspects of the EOD waveform. The dependence of the EOD amplitude, the amplitude of  $W(t)$ , on water resistivity or conductivity is displayed in (Fig. 19.4 B–C) and discussed below.

The model of the electric organ can be further refined (Hopkins, 1999): Let's assume each electrocyte of the organ generates a voltage  $V_c$  with inner resistance  $R_c$ . Note again, because of Thévenin's theorem, details of this model of an electrocyte do not matter as long as they behave linearly. The organ has  $m$  columns each of which contains  $n$  electrocytes. Because batteries and resistances in series add up, the total source voltage

$$V_s = nV_c \quad (19.9)$$

and the inner resistance

$$R_s = \frac{n}{m} R_c \quad (19.10)$$

are proportional to the number  $n$  of electrocytes per column. Higher numbers of parallel columns,  $m$ , increase the output current and reduce the inner resistance. By varying  $n$  or  $m$  the output voltage and the inner resistance can be adapted accordingly on evolutionary or seasonal time scales.

### Geometric spreading

By differentiation of Eq. (19.7) according to Eq. (19.3), we find the magnitude of the electric field of a dipole to be proportional to

$$|\vec{E}| \sim W(t) \frac{1}{r^3} \quad (19.11)$$

in any direction  $\alpha$ . It drops quickly with distance cubed (Fig. 19.3 C). At twice the distance EOD amplitude drops eightfold — almost one order of magnitude. A tenfold increase in distance reduces EOD amplitude by a factor of one thousand.



### Parameter influencing the far field

Both, the dipole potential and the electric far field of an electric fish, depend on the dipole moment  $P_V(t)$  and the inner conductivity  $\sigma_s$  of the electric organ as properties of the electric fish, and on the water conductivity  $\sigma_w$ . Note that all three parameters together only scale the dipole field via  $W(t)$ . They do not influence the power-law dependence on distance. For a given water conductivity, the waveform factor  $W(t)$  is a unique identifier of the EOD amplitude, since it is independent of the placement of measurement electrodes. It is not so easily deduced from measurements in a tank in comparison to a head to tail recording. However, by means of electrode arrays submerged in natural habitats it is even possible to deduce  $W(t)$  in natural habitats from unrestrained fish (Henninger, Krahe, Sinz, and Benda, 2020).

The dipole moment  $P_V(t)$  reflects the effective strength and the waveform of the electric organ discharge. Usually, the larger the fish, the larger its electric organ, and the larger the amplitude of its EOD (Knudsen, 1975; Westby and Kirschbaum, 1981; Hopkins, 1972; Hagedorn, 1988). A standardized estimate of the dipole moment could be used by the fish for an estimate of fish size (Knudsen, 1975), a proxy for its fitness (Hopkins, 1999; Gavassa, Silva, Gonzalez, and Stoddard, 2012).

### Effect of water conductivity

In essence, EOD amplitude (the amplitude of  $W(t)$ ) depends inversely on water conductivity (Eq. (19.8), Fig. 19.4 C, Harder, Schief, and Uhlemann, 1964). The lower the conductivity, the stronger the electric field amplitude. Vice versa, the higher the conductivity, the smaller the electric field amplitude, because the current source of the dipole is short circuited. This is a major factor explaining why an active electrosense developed in tropical freshwater fish only. Many streams and lakes in the tropics have very low conductivities (from few hundreds down to a few  $\mu\text{S cm}^{-1}$ , Crampton and Albert, 2006), much lower than in temperate zones (up to one thousand  $\mu\text{S cm}^{-1}$ ) or marine waters (ten thousands of  $\mu\text{S cm}^{-1}$ ). The same electric organ generating a head-tail voltage of 1 mV in a tropical stream would result in a voltage of approximately 1  $\mu\text{V}$  in the ocean. Indeed, *Gnathonemus petersii* fails to electrolocate in water approaching conductivities of 1000  $\mu\text{S cm}^{-1}$  (von der Emde, 1993). A consequence of the dependence of EOD amplitude on conductivity is that electrolocation and electrocommunication ranges moderately shrink with increasing conductivity, because of the down scaled field amplitudes (but see Escamilla-Pinilla, Mojica, and Molina, 2019). This effect seems to be amplified by an increased receptor threshold for higher water conductivities (Squire and Moller, 1982).

The exact dependence of EOD amplitude on water conductivity depends, according to Eq. (19.8), on the inner conductivity of the electric organ (Fig. 19.4 B–C). This dependence has been found to faithfully describe experimental data for both Gymnotiformes wave fish (Knudsen, 1975; Heiligenberg, 1975) and pulse fish (Caputi, Silva, and Macadar, 1998) as well as for Mormyridae (von der Emde, 1993). If the water conductivity matches the inner conductivity,  $\sigma_s = \sigma_w$ , the EOD amplitude is exactly half of its maximum possible value at zero water conductivity. This property can be used to measure the inner conductivity experimentally. For Apterodontidae and *Gnathonemus petersii* the inner conductivity is at approximately 100  $\mu\text{S cm}^{-1}$ , whereas for Sternopygidae and *Gymnarchus niloticus* it is approximately 17  $\mu\text{S cm}^{-1}$  (Knudsen, 1975; Heiligenberg, 1975; von der Emde, 1993), roughly matching conductivities of the natural habitats of the fish (Heiligenberg, 1975).

Different species of the genus *Brachyhypopomus*, gymnotiform pulse fish, are specialized in waters of different conductivities. They differ in width and length of their tails, reflecting different numbers of columns and electrocytes per column in their electric organs. Fish in higher water conductivity have more columns and less electrocytes per column, resulting in lower inner resistances, Eq. (19.10), potentially matching water conductivity of the habitats (Hopkins, 1999). This impedance match ( $\sigma_s = \sigma_w$ ), implies that for a given electric organ the amplitude of the EODs is at half their maximum possible value (Fig. 19.4 C), and that the power generated by the electric organ is maximal in comparison to conditions with higher or lower water conductivities (Fig. 19.4 D). This seems to imply that on evolutionary or seasonal time scales, the inner conductivity of the organ should adapt to the predominating water conductivity in a given habitat. As a function of the inner conductivity, however, the voltage, current and power output of the electric organ monotonically increase and there is no optimum (Fig. 19.4 E). A good compromise between a large enough EOD amplitude and low energetic costs might turn out to be close to an

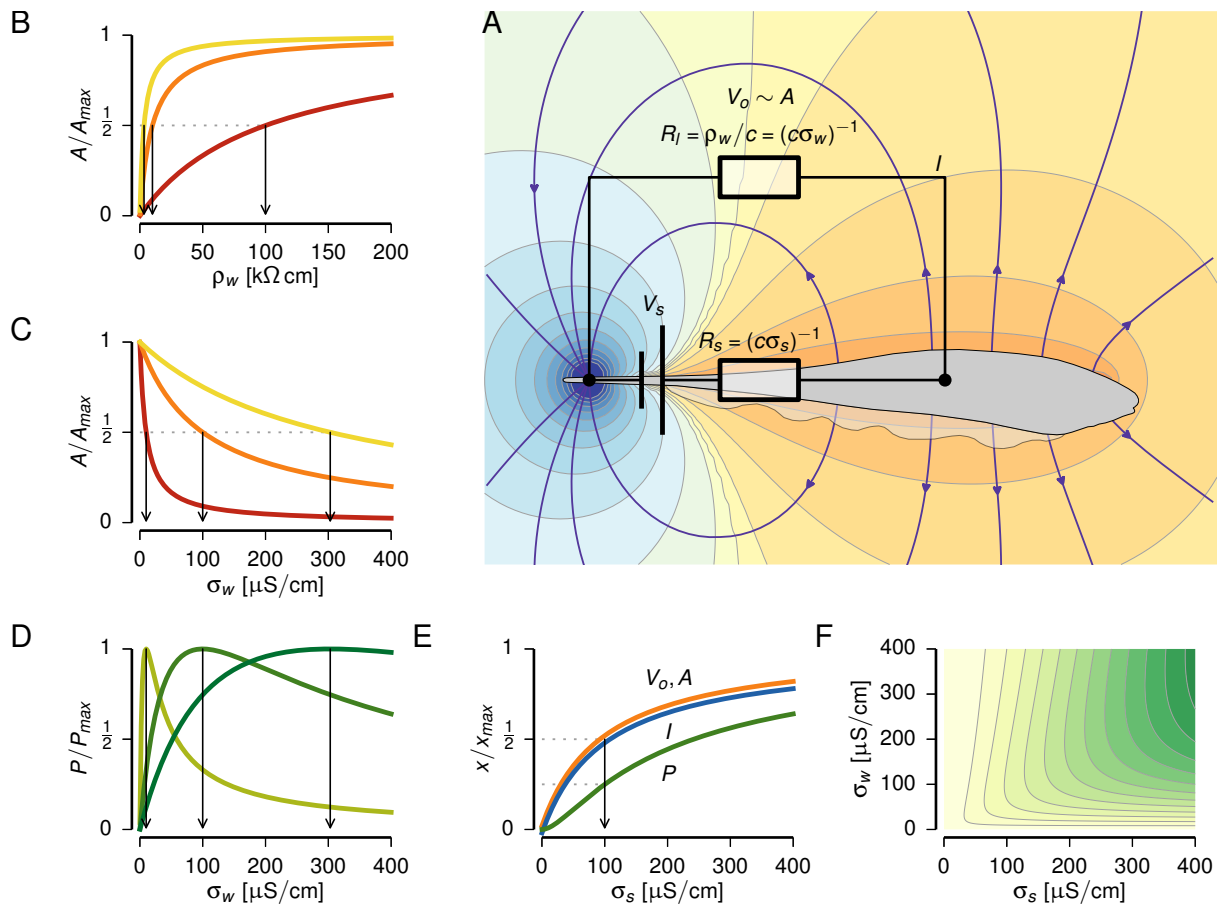


**Figure 19.4:** Electric organ model. **A** Any combination of voltage- and current sources is equivalent to a voltage source  $V_s$  with an inner resistance  $R_s$  in series. Connected to this is an effective load resistance  $R_l$  of the water surrounding the fish. The output voltage of the electric organ  $V_o$  generates a current  $I$ . **B** As a consequence,  $V_o$  and thus the amplitude  $A$  of the EOD waveform  $W(t)$  increase with increasing resistivity  $\rho = 1/\sigma_w = cR_l$  of the water according to Eq. (19.8).  $A_{max}$  is the maximum EOD amplitude obtained at infinitely large resistivity. The inner resistance  $R_s$  determines how quickly EOD amplitude rises with water resistivity. The EOD amplitude is half of its maximum value when the water resistivity matches the inverse inner conductivity  $\sigma_s = (cR_s)^{-1}$  (arrows at 10, 100, and 300  $\mu$ S cm $^{-1}$ ). **C** Same EOD amplitudes plotted against water conductivity  $\sigma_w = 1/\rho_w$  — the prevalent unit used in more recent literature. **D** For matching impedances,  $R_s = R_l$ , and thus for matching conductivities ( $\sigma_s = \sigma_w$ , arrows), the power output of an electric organ,  $P = R_l I^2$ , as a function of water conductivity is maximal for a given inner conductivity. **E** EOD amplitude  $A$ , (output voltage  $V_o$ , orange), current  $I$  (blue) and corresponding power  $P$  (green) are monotonically increasing functions of the inner conductivity (inverse inner resistance) for fixed water conductivity (arrow). **F** Power output of the electric organ as a function of both water conductivity  $\sigma_w$  and inner conductivity  $\sigma_s$ . Darker greens indicate larger powers. Panels D and E are vertical and horizontal cross-sections, respectively.

impedance match. Further research is needed to resolve the interplay between properties of the electric organ and environmental factors like water conductivity (Fig. 19.4 F).

In *Gnathonemus petersii* the first phase of the EOD waveform (Fig. 19.2 F) increases in amplitude with resistivity of the water as expected, Eq. (19.8). However, the second, negative phase, deviates from the model, suggesting non-linear, load dependent effects to be involved in discharging the rostral faces of the electrocytes (Bell, Bradbury, and Russell, 1976).

### Near field characteristics

Closer to the fish the electric near field deviates from an ideal dipole field (Fig. 19.1), because the electric organ is not a point dipole and the generated electric field is distorted by the fish's body. The field is stretched out around the head and is more concentrated at the tail of the fish. The zero potential plane curves backwards toward the tail (Heiligenberg, 1973; Knudsen, 1975; Caputi, Budelli, Grant, and Bell, 2000; Assad, Rasnow, and Stoddard, 1999). To a first approximation these effects can be accounted for by a line-charge model of the electric organ, and the length of the electric organ becomes an additional parameter in the equations describing the electric near field (Bacher, 1983). The near field geometry of the electric field is similar in Gymnotiformes and Mormyridae. Although in Mormyridae the electric organ is concentrated in a small tail region of the fish, the highly conductive body of the fish funnels the field rostrally (Caputi, Budelli, Grant, and Bell, 2000; Migliaro, Caputi, and Budelli, 2005). The near field can be quite well simulated by adding up the electric fields generated by monopoles arranged in a line, with the tail-most monopole charged oppositely to all the other ones (Chen, House, Krahe, and Nelson, 2005; Bacher, 1983). This is how the figures in this chapter were generated.

In many Gymnotiformes electrocytes are not discharged exactly at the same time along the electric organ (Rasnow and Bower, 1996; Rodríguez-Cattáneo<sup>1</sup>, Aguilera, Cilleruelo, Crampton, and Caputi<sup>1</sup>, 2013). Also, the generated waveform varies along the electric organ (Hopkins, Comfort, Bastian, and Bass, 1990; Caputi, 1999). Consequently, the temporal and spatial dependencies of the field strength are not independent anymore as in the dipole equation, Eq. (19.7). In some pulse-type Gymnotiformes, the near field is not necessarily rotational symmetric with respect to the body axis (Stoddard, Rasnow, and Assad, 1999; Assad, Rasnow, and Stoddard, 1999).

The particular properties of the near field play an important role for electrolocation, as discussed in the next section.

## 19.3 Electrolocation

By now we have discussed the properties of electric fields generated by single electric fish in infinitely large water bodies without any objects. Like any organism, electric fish need to interact with their environment — prey, predators, conspecifics, etc. The electric field produced by weakly electric fish is certainly not strong enough to be effective in stunning prey as the electric eels does. But it can be used to detect and localize objects. In his first study on *Gymnarchus niloticus*, Lissmann (1951) already suspected an electric sensing mode based on his observations of escape reactions to metal, but not to non-conducting rods and of attacks of playback electrodes. He later refined this hypothesis to the basics of electrolocation; electric fish sense distortions of the electric field induced by objects that differ in their conductivity from that of water (Lissmann and Machin, 1958).

An object placed in an external electric field gets polarized. That is, the electric field separates charges in the object and in this way induces a dipole density in the object. This dipole density then in turn generates its own electric field that superimposes with the external field. This polarization of objects is the effect electric fish utilize for electrolocation. Objects in the electric field get polarized and distort the field in specific ways (Fig. 19.5 A). These distortions are measured by electroreceptors on the skin of the fish and this information can be used to infer distance, size and electrical properties of the object causing the field distortions.

### 19.3.1 Perturbing field and electric image

For electrolocation the concepts of perturbing fields and electric images are central. Without any objects, the electric field generated by the electric fish is  $\vec{E}_{\text{basal}}(\vec{r})$  at position  $\vec{r}$  around the fish. This unperturbed field is also called the “basal field”. An object placed in the electric field of the fish gets polarized and distorts the basal field to  $\vec{E}_{\text{distorted}}(\vec{r})$ . The “perturbing field”,  $\vec{E}_{\text{perturbing}} = \vec{E}_{\text{distorted}} - \vec{E}_{\text{basal}}$ , is the difference between the distorted and the basal field. It is the electric field that is added by the object to the basal field (Lissmann and Machin, 1958).

The electrosensory system does not have access to the whole space around the fish. Electroreceptors can only measure the electric field at the body surface. They form a two-dimensional sensory array (Bennett, 1971), like a retina. Via the transdermal voltage, Eq. (19.4), electroreceptors measure the component of the electric field in

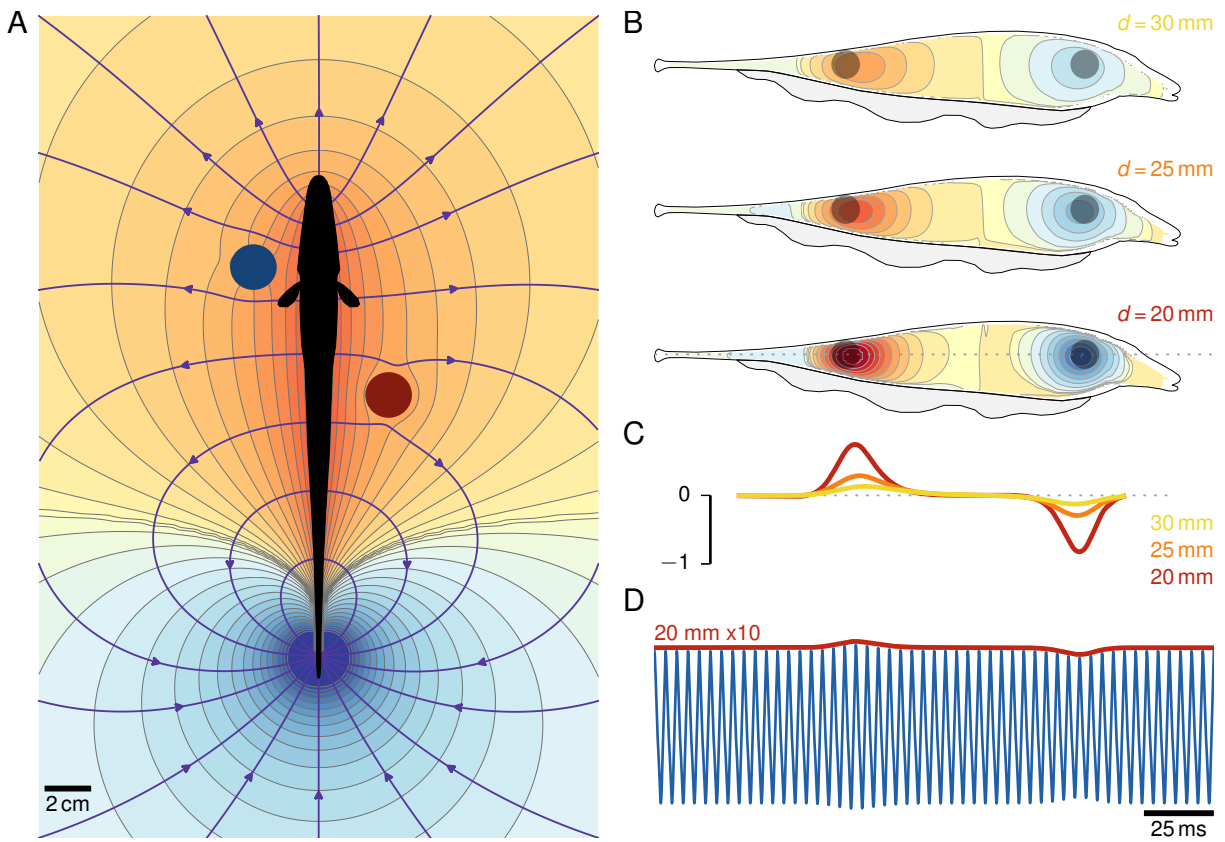


**Figure 19.5:** Electrolocation. **A** Objects distort the electric field. Isolators (blue sphere) push electric field lines (arrows) apart, whereas conductors (red sphere) attract them. **B** Electric images of a spherical conductor (left) and an isolator (right), both with radius of 6mm. The electric image is the change of a fish’s electric field induced by objects on the body surface of the fish. Isolators reduce the electric field, conductors increase it. The larger the distance  $d$  of the objects from the fish’s body axis the more blurry is the electric image. At a distance of 20 mm the spheres almost touch the body surface. Because of the curved field lines the peak of the electric image is not exactly aligned with the object’s position (parallax (Pedraja, Hofmann, Lucas et al., 2018)). **C** Cross-section of electric images shown in B along the midline given in percent of the unperturbed electric field. The conductor increases electric field amplitude whereas the isolator decreases it. The signals are small and quickly drop with distance. **D** To visualize the small effects of object signals on the fish’s EOD the curve from C with the largest response (closest distance) is multiplied by ten before modulating the EOD amplitude.

the direction they are pointing. The electric image,  $V_{\text{image}}(\vec{x})$ , is the transdermal voltage induced by the perturbing field at each position  $\vec{x}$  of the body surface (Fig. 19.5 B, Heiligenberg, 1975). Because of the linearity of Eq. (19.4) the electric image is the difference of the transdermal voltages of the electric field distorted by the object and the transdermal voltages  $V_{\text{basal}}(\vec{x})$  of the basal field. Note that the electric image is not just the potential of the field induced by the object at the skin; it rather is proportional to the electric field, Eq. (19.3), which is the spatial derivative of the potential. The waveform of the transdermal voltage of the distorted field,  $V_{\text{basal}} + V_{\text{image}}$  is referred to as the “local EOD”.

A convenient quantification of the electric image is the contrast of the electric image — the electric image relative to the unperturbed transdermal voltages (Lissmann and Machin, 1958). With Eq. (19.4) for the transdermal potential, image contrast

$$C_{\text{image}} = \frac{V_{\text{image}}}{V_{\text{basal}}} = \frac{\vec{E}_{\text{perturbing}} \cdot \vec{n}}{\vec{E}_{\text{basal}} \cdot \vec{n}} \quad (19.12)$$

reduces to the ratio of the projections of the perturbing and basal electric fields onto the receptor directions  $\vec{n}$ . All other details of the translation from electric fields to transdermal voltages cancel out.

The electric image is what the electrosensory system has to detect and evaluate in order to infer object position

and properties. For understanding electrolocation we need to know how electric images,  $V_{\text{image}}$  or  $C_{\text{image}}$ , look like, how they depend on object distance, size, shape, and electrical properties, and how these can be inferred from the electric image. Basically, electric images are shaped like a mexican hat, with a central peak right under the object, and a brim around it (Fig. 19.5 B, Hagiwara and Morita, 1963; Bastian, 1981; Bacher, 1983; Rasnow and Bower, 1996; Caputi, Budelli, Grant, and Bell, 2000; Gottwald, Bott, and von der Emde, 2017). Conductors attract field lines (red ball in Fig. 19.5 A) and thus increase electric field strength. The central peak of the electric image induced by conductors is positive. Insulators repel field lines (blue ball in Fig. 19.5 A) and thus induce negative electric images that reduce EOD amplitude. Electric image contrasts for small objects (less than a centimeter) are small, usually less than one percent (Fig. 19.5 C, D, Heiligenberg, 1973). The width of the electric image linearly increases with distance (Rasnow and Bower, 1996). As a result electric images get more blurry, i.e. smaller and wider, the further the object is away. Unlike visual systems that use lenses to focus an image onto a retina, the electrosensory system resembles a large retina that measures the images cast by objects that glow themselves without any optical apparatus (Budelli and Caputi, 2000). Electric fish use their self-generated electric fields to make objects glow, i.e. to polarize them.

### 19.3.2 Small spherical objects

In general, electric images for arbitrary objects cannot be computed analytically, instead numerical methods like finite elements and related methods need to be employed (Heiligenberg, 1975; Hoshimiya, Shogen, Matsuo, and Chichibu, 1980; Caputi, Budelli, Grant, and Bell, 2000; Babineau, Longtin, and Lewis, 2006). A well known exception is the perturbing field of a small sphere, which is a special but fundamental and insightful case (Lissmann and Machin, 1958; Bacher, 1983; Rasnow and Bower, 1996; Budelli and Caputi, 2000; Sicardi, Caputi, and Budelli, 2000; Chen, House, Krahe, and Nelson, 2005). Let us assume that the electric field of the fish,  $\vec{E}(\vec{r}, t)$  Eq. (19.11), is homogeneous at the place  $\vec{r}_s$  of the sphere. Then, the effect of the sphere on the electric field is that of a dipole field superimposed on the fish's field. For each frequency  $\omega$  the amplitude of the potential of this induced dipole reads

$$\phi_s(\vec{r}, \omega) = \chi(\omega) \cdot R^3 \cdot \vec{E}(\vec{r}_s, \omega) \cdot \frac{(\vec{r} - \vec{r}_s)}{|\vec{r} - \vec{r}_s|^3} \quad (19.13)$$

where  $R$  is the radius of the sphere and  $\vec{E}(\vec{r}_s, \omega)$  is the amplitude and phase of the fish's electric field at frequency  $\omega = 2\pi f$  in the sense of a Fourier decomposition. The electrical contrast

$$\chi(\omega) = \frac{\sigma_s - \sigma_w + i\omega(\epsilon_s - \epsilon_w)}{\sigma_s + 2\sigma_w + i\omega(\epsilon_s + 2\epsilon_w)} \quad (19.14)$$

is set by the conductivities  $\sigma_s$  and  $\sigma_w$  and permittivities  $\epsilon_s$  and  $\epsilon_w$ , of the sphere and the water, respectively (Rasnow and Bower, 1996).

Four different factors independently shape the electric image of the induced dipole, Eq. (19.13) (from back to front): (i) geometric spread of the induced dipole field back to the fish's body surface, (ii) amplitude and waveform of the EOD at the place of the sphere, (iii) the geometry (size and shape) of the sphere, and (iv) the electric properties of the sphere and the water via their electric contrast. The latter, in particular, is specific to electrosensory systems. Item (iii) and (iv) are properties of the object that together describe its ability to alter the fish's electric field. This interaction with the fish's field has been named "imprimence" by Lissmann and Machin (1958) (see chapter Caputi). Item (ii), EOD amplitude and waveform, is the active element. Without the electric field of the fish there is no electric image. Also, EOD waveform is the only species specific parameter in Eq. (19.13). All others are given by the physics of the problem and are the same for all species. In the following sections I discuss the properties of Eq. (19.13) and Eq. (19.14), compare them to experimental findings and finally address the inverse problem the fish have to solve.

Keep in mind that the induced dipole field, Eq. (19.13), is an approximation of the real situation. The electric field of an electric fish is not homogeneous. This, however, turns out to be a small problem even for not so small objects close to the fish (Rasnow and Bower, 1996). More important is the fact that the fish body itself also interacts with the perturbing field of the sphere (Pereira, Aguilera, and Caputi, 2012). This interaction is the reason



for the mexican hat profile of electric images (Caputi, Budelli, Grant, and Bell, 2000; Sicardi, Caputi, and Budelli, 2000), which is not sufficiently reproduced by the induced dipole of the sphere. Nevertheless, we can gain some fundamental insights into the electric world of electric fish from Eq. (19.13), that in their generality cannot be obtained from measurements or simulations.

### 19.3.3 Object distance

The amplitude of the electric image of the sphere, Eq. (19.13), is proportional to the electric field strength at the position of the sphere. In the far field, electric field strength drops according to Eq. (19.11) with distance cubed. The induced dipole field itself drops with distance cubed, too. Consequently, the amplitude of the electric image of small objects drops with distance to the power of six in the fish's far field. At twice the distance of the object from the fish, the amplitude of the electric image drops by a formidable factor of 64, almost two orders of magnitude. The physics of dipole fields with their dependence on distance cubed is not favorable for electrolocation. In contrast, sound intensity drops with distance squared, and consequently the intensity of a returned echo drops with distance to the power of four, resulting in reasonably large ranges for echolocation (Nelson and MacIver, 2006).

In the near field the situation is more favorable. Because of the elongated frontal lobe of the dipole, electric field strength initially decays with an exponent of unity, resulting in electric image strength to decay with distance with an exponent around four (Chen, House, Krahe, and Nelson, 2005; Pereira, Aguilera, and Caputi, 2012). Still, the effect of a spherical object decays really quickly with distance (Fig. 19.5 B–D). For the same reason, the electric image of longer objects that could be approximated by a dipole line should decay with distance with even smaller exponents (Bacher, 1983).

These power law dependencies of electric images on distance have profound consequences for the detection range of objects. At distances beyond the near field, dramatic increases in electric organ strength are required for minor extensions of detection ranges. Indeed, electrolocation of small objects like prey items or artificial cubes or spheres is confined to the near field or less, depending on object size, as has been shown by numerous behavioral and modeling studies (Heiligenberg, 1975; Bastian, 1981; Nelson and MacIver, 1999; Schwarz and von der Emde, 2001; Snyder, Nelson, Burdick, and MacIver, 2007; MacIver, Patankar, and Shirgaonkar, 2010; Pereira, Aguilera, and Caputi, 2012; Pedraja, Aguilera, Caputi, and Budelli, 2014).

Because of fundamental physical laws there is no possibility of the fish to modify the dipole properties of the far electric field. But they can and did modify their near field. A low body resistance funnels the field along their body, resulting in collimated field lines perpendicular to the body surface (Castelló, Aguilera, Trujillo-Cenóz, and Caputi, 2000; Migliaro, Caputi, and Budelli, 2005; Sanguinetti-Scheck, Pedraja, Cilleruelo et al., 2011). As a result the exponent governing the power law decay of the electric field is significantly reduced. For electrolocation the electric sense operates within the near field.

In Mormyridae the EOD waveform is the same at any position around the fish, because of their compact electric organ that is discharged simultaneously. In Gymnotiformes the electric organ is much longer and stretches through most of the body. In some Gymnotiformes the electric organ is discharged in complex ways. As a consequence, EOD waveform in many Gymnotiformes changes along the body (Pedraja, Aguilera, Caputi, and Budelli, 2014). The waveform of the electric image is that at the position of the object superimposed on the EOD waveforms along the skin, which might be a different one. In this case, EOD waveform already contains information about object position (Pedraja, Aguilera, Caputi, and Budelli, 2014).

### 19.3.4 Object size and shape

How does object size and shape influence electric images? According to Eq. (19.13) the radius cubed or simply the volume of the sphere only scales the electric image, it does not distort the profile of the image (Rasnow and Bower, 1996; Chen, House, Krahe, and Nelson, 2005). Doubling sphere radius increases the amplitude of the electric image everywhere by a factor of eight. The other way around, this dependence makes electric images of small objects really small. This seems to be similar for cylindrical objects (Heiligenberg, 1975) or cubes (von der Emde, 1998).



Non-spherical objects can be approximated by dipole lines and thus by a superposition of the elementary fields of small spheres (Bacher, 1983). The wider an object the wider and higher its electric image, but its peak flattens out (Sicardi, Caputi, and Budelli, 2000). Objects of similar dimensions but different shapes (e.g. spheres and cubes) result in similar electric images once the object is more than twice its major dimension distant from the fish. Only when they are closer do they give rise to different electric images (Sicardi, Caputi, and Budelli, 2000; Fujita and Kashimori, 2019). Equivalently, spatial electroacuity, the minimum distance between two objects to result in discriminable electric images, increases with object distance and decreases with object size (Babineau, Longtin, and Lewis, 2007).

### 19.3.5 Conductive objects

In general, the electrical contrast, Eq. (19.14), is complex valued and depends on the frequencies of the driving EOD. We deal with that in the next section on capacitive objects. More generally, the electric contrast actually is a polarization tensor describing the intrinsic geometric and electric properties of an object (Ammari, Boulier, Garnier, and Wang, 2014). Here we discuss the simplest case of purely conductive objects with real valued and frequency independent electric contrasts. In the same way as the size of the sphere, the conductivity of such objects just scales the driving EOD waveform  $\vec{E}(\vec{r}_s, t)$  and the electric image without distorting it (Caputi, Budelli, Grant, and Bell, 2000).

For conductive objects with permittivities similar or smaller than that of water,  $\omega\epsilon$  is small in comparison to typical values of the water conductivity and thus can be neglected. For such conductive objects the electric contrast depends solely on the conductivity of the object relative to the one of water:

$$\chi(\omega) = \frac{\sigma_s/\sigma_w - 1}{\sigma_s/\sigma_w + 2} \quad (19.15)$$

(Fig. 19.6 A, Lissmann and Machin, 1958). For perfect conductors (metal spheres) with large values of  $\sigma_s$ , the electric contrast approaches unity. Metal objects add to the fish's EOD and thus have positive electric images. For perfect insulators with vanishing  $\sigma_s$ , the contrast approaches  $-1/2$ . Plastic spheres and rocks get subtracted from the fish's EOD and thus have negative electric images.

### 19.3.6 Capacitive objects

Electrical properties of biological tissues and materials are often characterized by extremely high permittivities in comparison to the one of water ( $\epsilon_w = 7.1 \text{ pF cm}^{-1}$ ). The permittivity quantifies capacitive properties of materials, that, in contrast to conductivity, not only scale electrical signals but also distort waveforms by introducing frequency dependent gains and phase shifts. Muscle tissue, for example, is approximately 10 000 times more permissive than water (Schwan, 1963). For objects relevant to electric fish only thin leafs of two species of water plants have been measured with similar results (up to  $\epsilon = 850 \text{ nF cm}^{-1}$  and a conductivity of  $\sigma \approx 10 \text{ } \mu\text{S cm}^{-1}$ , Heiligenberg, 1973). Indirect measurements by von der Emde (1990) match these values for plants, and hint at similar or smaller values for little fish. Weakly electric fish mainly feed on aquatic invertebrates, with chironomid larvae being the most important food source of many electric fish species (Winemiller and Adite, 1997). These have been reported to have conductances of  $2 \text{ } \mu\text{S}$  and small capacitances in the range of  $1 \text{ nF}$  (von der Emde and Ringer, 1992).

Conductivity, together with permittivity, define the electrical contrast, Eq. (19.14), which is a filter that applies a gain and a phase shift to each frequency component of the fish's electric field at the position of the object. How a specific object filters the EOD depends according to Eq. (19.14) on its conductivity and permittivity in relation to the ones of the surrounding water (Lissmann and Machin, 1958; Bacher, 1983).

Purely capacitive objects with a capacity  $C$  between two electrodes separated by some distance  $d$  have zero conductivity and their permittivity equals  $\epsilon_s = C/d$ . Whereas in electrical circuits the impedance of a capacitor is inversely proportional to the frequency and the capacitance, the effect of a capacitor on the electric image is given by the electric contrast, Eq. (19.14), where the capacity enters both the numerator and the denominator via the permittivity, and thus saturates for both low and high frequencies (Fig. 19.6 B). The electric contrasts of capacities

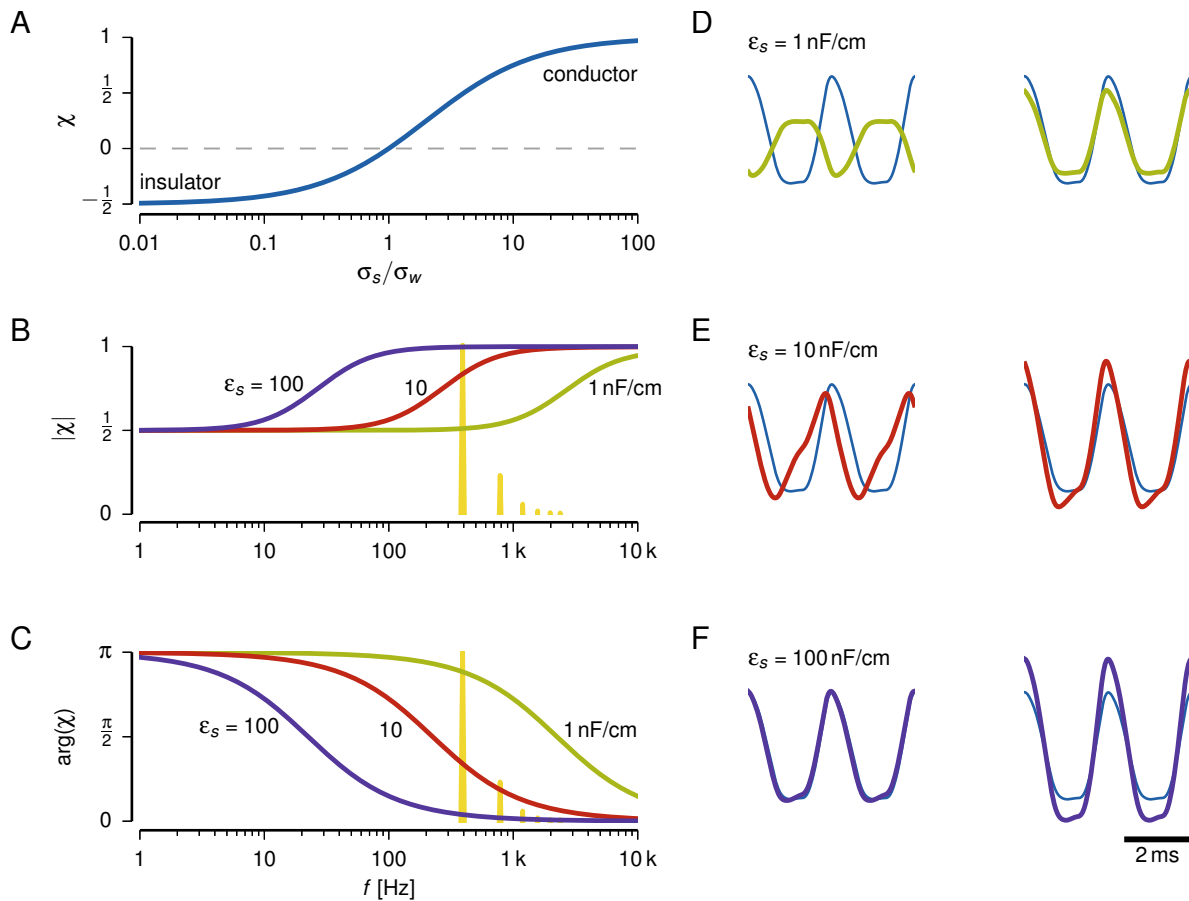


**Figure 19.6:** Electric contrast. **A** Purely resistive objects simply scale the local EOD waveform. Insulators with conductivities much lower than the one of water invert the EOD waveform (like in panel D), because they result in a negative electric contrast  $\chi$ . The electric contrast of conductors with conductivities much larger than that of water are positive and twice as large than the one for perfect insulators (panel F). **B** Capacitive objects modify the EOD waveform in a frequency dependent way. The gain  $|\chi|$ , by which the local EOD waveform is modified, rises in a sigmoidal way from one half to one and the frequency of the transition scales with the inverse permittivity  $\epsilon_s$  of the object as indicated and with water conductivity (here  $\sigma_w = 10 \mu\text{S cm}^{-1}$  is used). The effect on EOD waveform is largest, when the amplitude spectrum of the EOD (yellow, *Eigenmannia* with  $\text{EOD}f = 400 \text{ Hz}$ ) falls into this transition region. **C** The phase shifts corresponding to the gains shown in B as introduced by capacitive objects. **D–F** The effect of frequency dependent electric contrasts of capacitive objects on the EOD waveform of the electric image (left column) and the local EOD somewhere near the object (right column), that is the unperturbed EOD (thin blue lines) plus the electric image waveform. An *Eigenmannia* EOD waveform of 400 Hz is shown as an example. **D** For too low object permittivities, the effect of a capacitive object approaches that of an insulator. The EOD waveform is halved and inverted because of the phase shift of  $\pi$ . **E** For Intermediate permittivities, where the EOD spectrum falls into the transition regions of gain and phase shift, the modulating effect on EOD waveform is largest. **F** For object permittivities too high in relation to the EOD spectrum, the effect resembles that of a conductor. EOD waveform is simply scaled, because the gain is unity and the phase shift is zero.

that are small in relation to the EOD's power spectrum approach that of insulators, whereas high capacities resemble conductors (Budelli and Caputi, 2000; Caputi, Castelló, Aguilera et al., 2008). One may wonder whether the well known escape responses of weakly electric fish to metal objects (Lissmann, 1951) is triggered because the fish are not used to metal objects or because of electrochemical currents (Lissmann and Machin, 1958), or whether metal objects are perceived as objects with high capacities or conductances that might hint at predatory fish (see Fig. 7 in von der Emde, 1990, or Fig. 2A in Gottwald, Singh, Haubrich, Regett, and von der Emde, 2018). Only for intermediate capacities does the electric contrast become complex and modulate the EOD waveform by frequency dependent phase shifts (Fig. 19.6 B & C). For purely capacitive objects the electric contrast solely depends

on  $\omega\epsilon_s/\sigma_w$ . Decreasing frequency,  $\omega$ , or permittivity of the object,  $\epsilon_s$ , or increasing water conductivity,  $\sigma_w$ , simply shifts the electric contrast to higher values on logarithmic capacity, permittivity or frequency axes.

Amplitude and waveform modulations of the electric images and the EOD measured on the skin can be well explained by the properties of the electric contrast, Eq. (19.14), (Fig. 19.6 D–F), and are necessarily similar for both pulse and wave fish in Gymnotiformes and Mormyridae: (i) amplitude increases with capacity (von der Emde, 1990, 1998; Budelli and Caputi, 2000; Fujita and Kashimori, 2010), (ii) waveform changes are largest around intermediate values of the capacity (von der Emde, 1990, 1998; Budelli and Caputi, 2000; Fujita and Kashimori, 2010) that (iii) match the power spectrum of the EOD (Bacher, 1983; von der Emde and Ringer, 1992), and (iv) increasing water conductivity shifts these effects to higher capacity values (von der Emde, 1993; Rasnow and Bower, 1996).

In behavioral experiments electric fish reliably discriminate intermediate capacitances from resistive objects of any value (von der Emde, 1990; von der Emde and Ringer, 1992), indicating that they perceive the corresponding waveform distortions as a separate sensory quality (von der Emde and Ronacher, 1994), like another electric “color” (Budelli and Caputi, 2000) (see chapter Caputi). Against an insulator, capacities must be sufficiently large, and against conductors, capacities must be sufficiently small to be discriminable by the fish (von der Emde, 1990; von der Emde and Ringer, 1992; von der Emde, 1998), because low capacities look like insulators (Fig. 19.6 D) and high capacities like conductors (Fig. 19.6 F). Detection thresholds indeed change as expected from Eq. (19.14) with water conductivity (von der Emde, 1993) and with the power spectrum of the EOD waveform (Meyer, 1982; von der Emde and Ringer, 1992).

For intermediate capacities, electric contrast gets complex valued and filters EOD waveform, providing a cue for object capacity independent of electric image amplitude. In case of the biphasic waveform of *Gnathonemus petersii* (Fig. 19.2 F), the effect of this filtering operation can be readily quantified as the P/N ratio, the ratio between the amplitudes of the positive and negative peaks (von der Emde, 1990). Note that the result of the filtering operation of the electric contrast on the EOD waveform, and thus of the P/N ratio of the electric image is independent of distance and object size and solely depends on capacity. However, the P/N ratio is measured on the local EOD, i.e. the electric image added to the basal EOD waveform. The smaller the electric image amplitude, the smaller the waveform distortion the electric image exerts on the local EOD. As a result, P/N ratio is linearly related to electric image amplitude and the slope of this relation is a unique indicator of object capacity (Budelli and Caputi, 2000; Gottwald, Bott, and von der Emde, 2017) and can be used to discriminate different types of natural objects (Gottwald, Singh, Haubrich, Regett, and von der Emde, 2018). Amplitude and P/N ratio span a two-dimensional space of electric color (Budelli and Caputi, 2000) that reflects the perceptual independence of conductivity and capacity of electric fish (von der Emde and Ronacher, 1994). In electric fish with more complex EOD waveforms alternative measures to the P/N ratio might be used, for example spectral measures (Aguilera and Caputi, 2003). Even for EOD waveforms with more than two peaks, the electric color space cannot be more than two-dimensional, because electric contrast is a linear filter depending on the two quantities conductivity and permittivity, and because electric fish have exactly two sensory channels to evaluate local EOD waveforms.

### 19.3.7 Inferring object properties from electric images

During electrolocation objects cast electric images on the sensory surface made up of an array of electroreceptive organs on the skin of the fish. From the information given by electric images the fish needs to infer position and distance as well as geometrical and electrical properties of an object.

Rostrocaudal and dorsoventral location could be inferred directly from the location of the peak of electric image (Rasnow and Bower, 1996), taking the direction of the field lines into account (Bacher, 1983). An object at a given distance gives rise to an electric image with a mexican hat profile. Because objects size and electric contrast both enter the induced dipole field, Eq. (19.13), multiplicatively, they simply scale the image profile. Evidently, peak amplitude of the electric image is not an estimator for object distance; it is confounded by object size and electric contrast (Caputi, Budelli, Grant, and Bell, 2000; Budelli and Caputi, 2000). Normalizing the image profile by peak amplitude results in the same profile independent of image size and contrast. The width of such a normalized profile increases linearly with the distance of the object. Thus, object distance could be estimated by the width of

the electric image measured at a certain height relative to peak amplitude (Rasnow and Bower, 1996; Chen, House, Krahe, and Nelson, 2005) or from other properties like zero crossings (Bacher, 1983). Insulators can be easily distinguished from conductors based on the sign of the electric image (Fig. 19.6 A). Despite this, size and the value of the conductivity of small spherical objects cannot be separated; a less conductive object should be confused with a smaller object by the fish. Only capacitive properties can be estimated independently by means of P/N ratios as discussed above.

For larger non-spherical objects the relative width of the electric image also scales with object size (Bacher, 1983; Sicardi, Caputi, and Budelli, 2000) and therefore cannot be used as an estimate for object distance. Empirically, it turns out that the maximum slope of the EOD profile relative to its peak amplitude (slope amplitude ratio, SAR) is the only estimator of distance that is independent of object size and conductance or capacitance (von der Emde, Schwarz, Gomez, Budelli, and Grant, 1998; Gottwald, Bott, and von der Emde, 2017). However, even the SAR depends on object shape for close by objects (Sicardi, Caputi, and Budelli, 2000). This indeed results in an electric illusion that fish perceive cubes as being closer than spheres of the same size (von der Emde, 1998; Schwarz and von der Emde, 2001). Interestingly, moving plants behind an object improve object detection (Babineau, Longtin, and Lewis, 2007; Fechner and von der Emde, 2013).

### 19.3.8 Active sensing

As we just have discussed, disentangling distance from size and electric contrast based on single static electric images is difficult and even impossible. The way out of this dilemma is that the fish need to move in order to generate a sequence of images from which more detailed information can be extracted (Ammari, Boulier, Garnier, and Wang, 2017; Fujita and Kashimori, 2019).

Tail bending is a common behavior of electric fish that contributes to generate multiple electric images. In particular gymnotiform fish commonly bend their tail back and forth when exploring objects (Heiligenberg, 1975). The dependence of electric image amplitude on bending angle could be used as a unique cue for lateral distance independent of object size (Sim and Kim, 2011). Two nearby objects can be better discriminated if the tail is bend toward or around the objects (Heiligenberg, 1975; Babineau, Longtin, and Lewis, 2007). Equivalently, *Gnathonemus petersii* moves its finger like chin appendage, its Schnauzenorgan, in a saccade-like manner. The electric field is funneled into the Schnauzenorgan which is densely packed with receptor organs. The movements of the Schnauzenorgan illuminate objects in different ways and help to resolve ambiguities (Pusch, von der Emde, Hollmann et al., 2008).

In prey capture and object exploration behaviors electric fish often scan along an object (Nelson and MacIver, 1999). This leads to temporally changing transdermal voltages received by electroreceptors and the rate of change at a given receptor is a size invariant estimate of object distance (Hofmann, Sanguinetti-Scheck, Gómez-Sena, and Engelmann, 2013). Moreover, while approaching an object, *Gnathonemus petersii*, aligns its movement trajectory with the timing of its EODs such that the resulting relative electric flow (relative difference in electric image amplitude) becomes a size and conductivity independent measure of distance (Hofmann, Sanguinetti-Scheck, Gómez-Sena, and Engelmann, 2017).

### 19.3.9 Passive electrolocation

Electric organs of electric fish are not the only biotic sources of electric fields. Any organism generates electrochemical gradients that result in electric fields that can be measured in their vicinity. Fish, insect larvae and snails generate stationary dipole fields of substantial amplitudes in the millivolt range that are modulated by respiratory movements of the mouth or gills, in case of fish, and are particularly large at wounds (Roth, 1972; Peters and Bretschneider, 1972). These potentials are not of muscular origin, because they persist in freshly killed animals (Kalmijn, 1974). Muscle activity in fish generates non-stationary electric signals of a few milliseconds duration (Burham, Huckaby, Gowdy, and Burns, 1969). For more details on stimuli relevant for passive electrolocation see [chapter Chagnaud](#).

## 19.4 *Electronavigation*

As argued above, electrolocation of small objects is confined to the near field of the fish's electric field, because of the dipolar nature of polarization fields induced in small objects. However, the habitat of weakly electric fish is made up of many more objects than tiny prey items, many of them larger than the body size of the fish, like rocks, tree trunks, and the water surface. Because of their extended shapes, the polarization field of such objects does not drop like that of a dipole with distance cubed but with smaller exponents (Chen, House, Krahe, and Nelson, 2005). In addition, because of their size, they have a large impact on the fish's electric field. Large objects should thus make up important signals that potentially can be detected beyond the near field and be used for navigation.

### 19.4.1 *Nonconducting boundaries*

To understand how large objects influence the electric field, consider a planar nonconducting boundary. The water surface is such a boundary, but the surface of rocks and maybe tree trunks could be approximated by a nonconducting boundary as well. Isopotential planes go perpendicularly into such boundaries, the components of the electric field vectors perpendicular to the surface vanish. How does the fish's electric field change in the presence of nonconducting boundary?

The resulting electric field can be computed by mirroring the electric fish to the opposite side of the boundary and simply adding its electric field to the one of the original fish (method of image charges). The perturbing field is simply the electric field of the mirrored fish. The amplitude of the electric image is given by geometric spread of the mirrored fish's dipole field, Eq. (19.11), at twice the distance from the boundary. Unlike the devastating exponent of six governing the decay of electric image amplitudes with distance for small objects, the perturbing field of a planar nonconducting boundary drops with a benevolent power of three. This places the electrolocation of large objects into a completely different physical regime, and suggests detectability of large objects way beyond the near field regime.

Electric images of large nonconducting objects more closely resemble an electrocommunication situation, but with doubled distances (see next section). The temporal waveform of the mirrored fish and its EOD frequency, however, are exactly the same as the one of the real fish. The amplitude of the electric image can be much larger than the ones for small objects. The closer the fish to the boundary, the stronger the electric image, eventually reaching the full EOD amplitude at the skin of the fish. Such large effects of nonconducting boundaries have been verified experimentally (Chen, House, Krahe, and Nelson, 2005; Fotowat, Harrison, and Krahe, 2013).

### 19.4.2 *Effect of water depth*

In between two nonconducting boundaries at the top and the bottom of an electric fish, its electric field is compressed (Fig. 19.7 A). In natural habitats, the water surface is a prominent nonconducting boundary, whereas the bottom of the stream or lake might also approximate such a boundary, depending on its properties (Fig. 19.7 B). The compression of the field considerably reduces the exponent of the power law dependence of the electric field strength on distance (Fotowat, Harrison, and Krahe, 2013; Henninger, Krahe, Sinz, and Benda, 2020). Within about one body length, these two boundaries strongly increase electric image amplitude frontal and lateral to the fish, but decrease it dorsally and ventrally (Fig. 19.7 C). Even for larger distances between the boundaries, a significant signal remains frontal to the fish. Thus, water depth or the fish's distance from the water surface could be an easily detectable cue for electronavigation. Similar strong effects are to be expected for fish hiding in crevices or swimming between close by rocks.

### 19.4.3 *Passive electronavigation*

In addition to active electronavigation that relies on the fish's self-generated electric field, passive electronavigation is based on low frequency electric fields of abiotic origin present in the environment that could be sensed by the fish's passive (ampullary) electrosensory system (see chapter Chagnaud). A number of sources potentially available for navigation have been suggested early on. Unfortunately no progress has been made regarding the



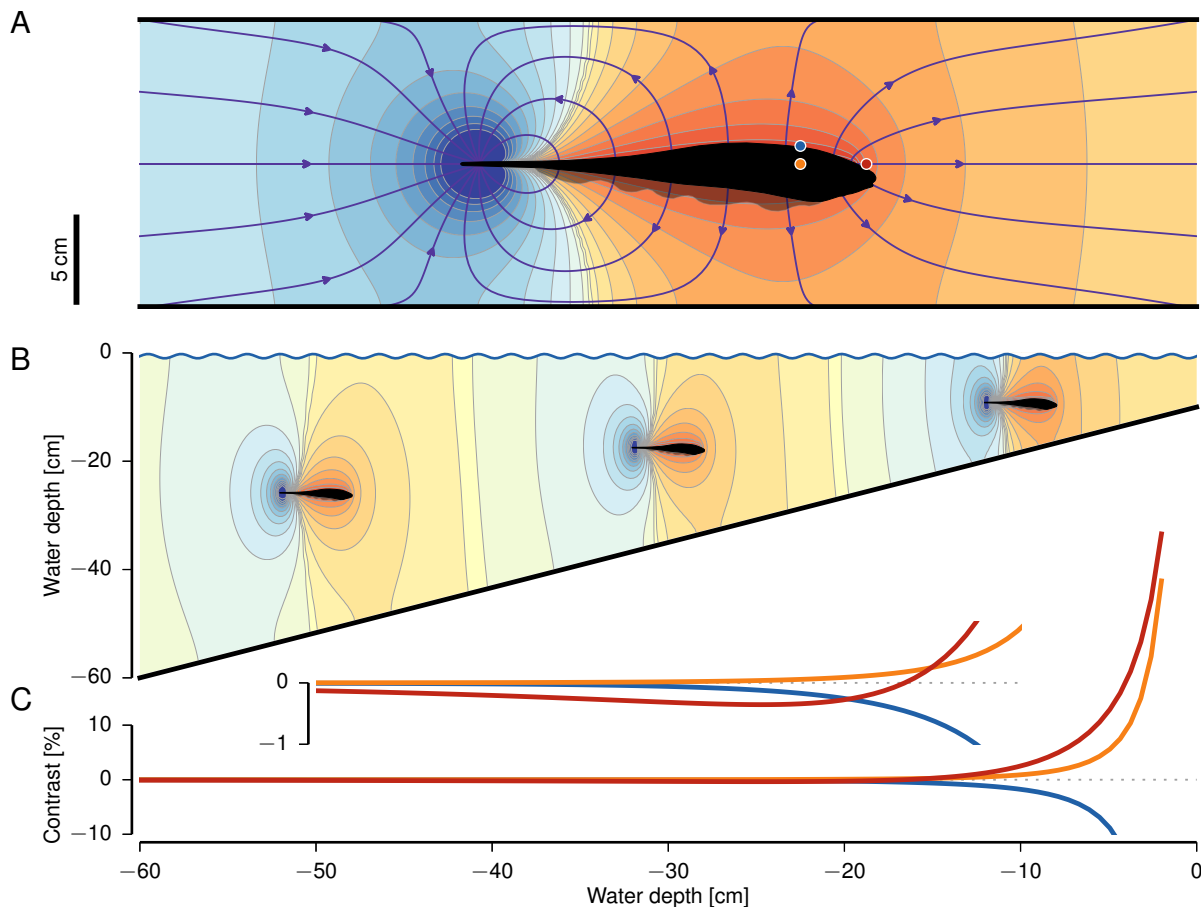


**Figure 19.7:** Electronavigation. **A** Planar nonconducting boundaries (black lines) compress the electric field lines (blue arrows). **B** The water surface (blue) and the ground (black) at some water depth are such boundaries. **C** Consequently, water depth is a strong electric signal in shallow waters (one body length). Field amplitude is increased frontal (red) and lateral (orange) of the fish and decreased dorsally (blue) and ventrally. But even in deeper waters a significant signal remains in frontal directions (inset) that could be used for navigation.

magnitude, frequencies, stabilities and usabilities of these sources for tropical freshwater fishes with ampullary systems, including electric fishes.

Water moving through the earth's magnetic field induces an electric field perpendicular to both the direction of the moving water and the magnetic field (Lissmann and Machin, 1958; Kalmijn, 1974). Close to the magnetic equator where magnetic field vectors point horizontally, a vertical electric field would only be generated by the east-west component of a water flow. The resulting electric field distribution within and along a river could provide navigational cues in addition to information on water speed conveyed by the lateral line system (see chapter Montgomery).

Another interesting source of electric fields are streaming potentials of electrochemical origin resulting from rivers and streams flowing over different geological formations in their beds or along their banks (Kalmijn, 1974). These would provide information about chemical non-uniformities in the river bed and could be used as cues for orientation. *Gnathonemus petersii* can discriminate metal from plastic rods even without active electrolocation (Belbenoit, 1970). Peters and Bretschneider (1972) measured hydroelectric fields of unknown origin in European ponds that were fairly constant in strength and direction.

Electric fish and catfish can be trained on the presence and direction of weak static electric fields (Kalmijn, 1974) and on the presence of static magnetic fields (Lissmann and Machin, 1958). So in principle, the mentioned cues could be used by electric fish.



## 19.5 Electrocommunication

Let us now turn to the interaction between electric fish. By emitting an electric field they provide a notable stimulus to other electric fish, both conspecific and allospecific. In contrast to electrolocation, electrocommunication involves only a single dipole, the one describing the field of the emitting fish. Electric field strength decays with distance cubed. This much lower exponent governing the decay of electrocommunication signals with distance results in communication ranges of up to 2 m (Henninger, Krahe, Sinz, and Benda, 2020), clearly more than the near field of a fish and associated typical electrolocation ranges (Knudsen, 1975). Indeed we observed turning and attacking an intruding male at distances up to 2 m in the wild (Henninger, Krahe, Kirschbaum, Grewe, and Benda, 2018). The exact maximum communication range is of course species dependent, as the EOD amplitude varies considerably between species (Pedraja, Aguilera, Caputi, and Budelli, 2014).

The emitted EODs and EOD frequency already communicate species identity, sex, and social status (Hopkins, 1974a; Dunlap and Oliveri, 2002; Fugère, Ortega, and Krahe, 2011; Raab, Linhart, Wurm, and Benda, 2019; Henninger, Krahe, Sinz, and Benda, 2020). Most interestingly, electric fish can also modulate the frequency and amplitude of their EODs. This way they generate various types of communication signals like chirps and rises that they use to actively communicate with each other (Zakon, Oestreich, Tallarovic, and Triefenbach, 2002). These signals are used in courtship and to synchronize spawning (Hagedorn and Heiligenberg, 1985; Henninger, Krahe, Kirschbaum, Grewe, and Benda, 2018) and in aggressive contexts (Hupé, Lewis, and Benda, 2008; Triefenbach and Zakon, 2008).

Let's start with beats arising between two stationary fish. For electrocommunication beats are what small spheres are for electrolocation. They are the essence of any signals arising in electrocommunication contexts. Beats between moving fish give rise to motion envelopes. The various types of electrocommunication signals temporarily modify the beat pattern in specific ways.

### 19.5.1 Wave fish beats

Wave fish continuously emit EODs. Whenever two wavefish come close to each other, their EODs inevitably superimpose (Fig. 19.8 A) and result in a periodic amplitude modulation, a so called “beat” (Fig. 19.8 B). The receiving fish senses its own electric field with frequency  $f_1$  with some amplitude  $A_1$  (Fig. 19.8 B top). The electric field of another fish in general has a different frequency  $f_2$  and, at the position of the receiving fish, a smaller amplitude  $A_2$  (Fig. 19.8 B center). At times where the two EOD waveforms are in phase, peaks of the other fish add to peaks of the receiving fish. Whenever the two waveforms are antiphase, troughs of the other fish subtract from peaks of the receiver. The phase relation between the two EODs changes periodically with the beat period resulting in a periodic waxing and waning of the EOD amplitude (Fig. 19.8 B bottom).

#### Beat amplitude

The amplitude of the beat equals the amplitude  $A_2$  of the other fish at the position of the receiving fish. According to the dipole field, Eq. (19.1), the amplitude inversely depends on distance cubed and on the orientation of the fish relative to each other. Often, beat amplitude is quantified relative to the amplitude of the receiving fish as the beat contrast  $C = A_2/A_1$ . The stronger the beat contrast the deeper the amplitude modulation (Fig. 19.8 C). Beat contrast is equivalent to electric image contrast, Eq. (19.12), in electrolocation.

#### Beat frequency

The inverse of the beat period is the beat frequency  $|\Delta f|$ . It equals the absolute value of the difference frequency  $\Delta f = f_2 - f_1$  between the EOD frequencies of the two fish. The higher the beat frequency, the faster the amplitude modulation (Fig. 19.8 D). In *Apteronotus rostratus*, for example, with EOD frequencies ranging from 600 to more than 1000 Hz, beat frequencies range from 0 to 250 Hz for male-male interactions, and up to more than 400 Hz for male-female interactions because of their sexual dimorphism in EOD frequency (Henninger, Krahe, Kirschbaum,

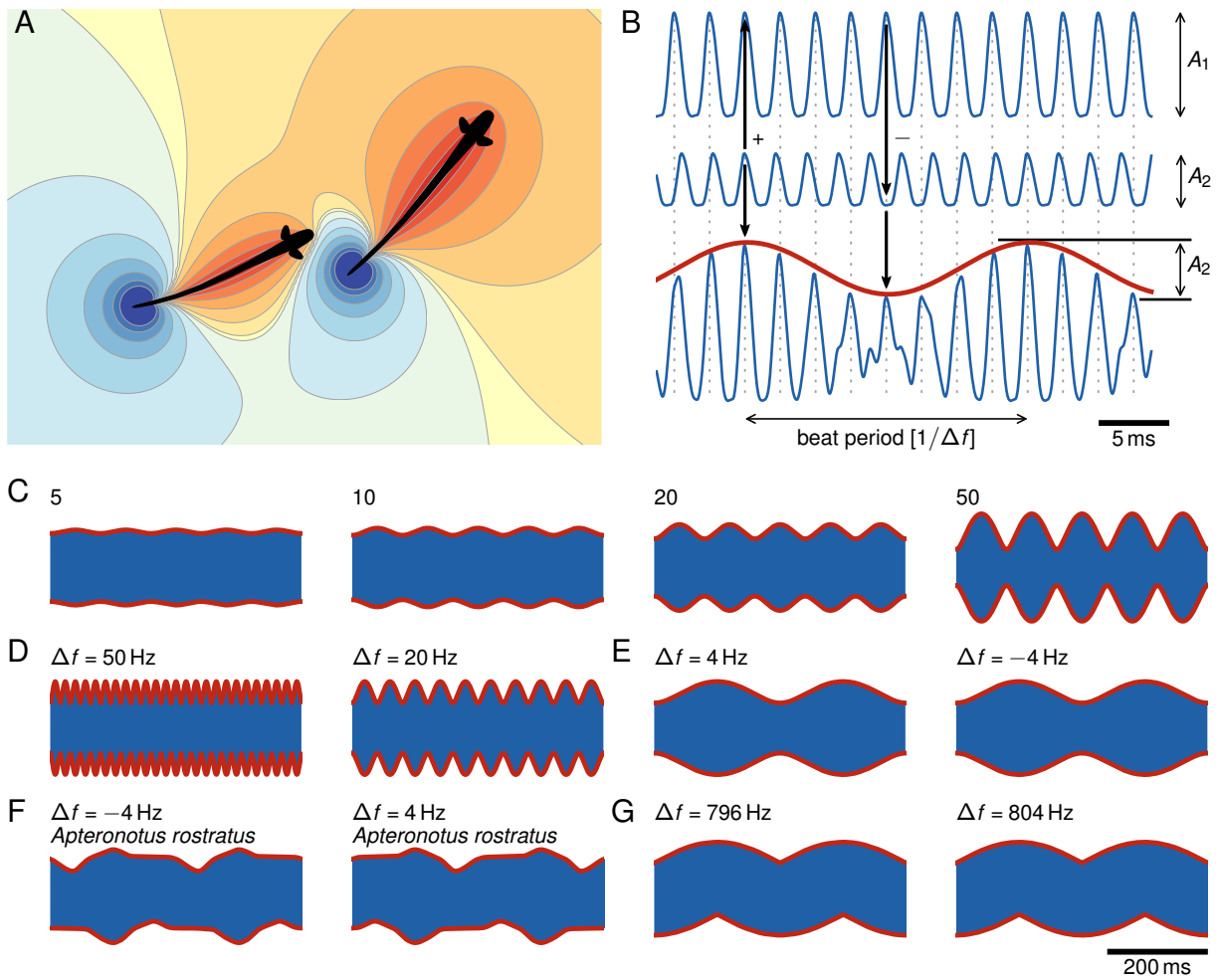


**Figure 19.8:** Beats of wave-type electric fish. **A** EODs of wave-type electric fish superimpose continuously. **B** The EOD of the receiving fish (top) with amplitude  $A_1$  and EOD frequency  $f_1$  superimposes with the EOD of the other fish (center) with another frequency  $f_2$  and an amplitude  $A_2$  that is usually smaller than  $A_1$  because of the decay of the electric field with distance. The resulting waveform (bottom) is a periodic amplitude modulation (red), called “beat”, with amplitude  $A_2$  and frequency given by the difference frequency  $\Delta f = f_2 - f_1$ . **C** Beat contrast is the amplitude  $A_2$  of the beat relative to the amplitude  $A_1$  of the unperturbed EOD of the receiving fish. It is a measure of the modulation depth of the beat. **D** The higher the beat frequency, the absolute value of the difference frequency  $\Delta f = f_2 - f_1$ , the faster the beating amplitude modulation. **E** When using sinusoidal EOD waveforms the amplitude modulation is the same for both positive and negative difference frequencies. **F** With real EOD waveforms the beat waveform resembles the EOD waveform and the symmetry of positive and negative difference frequencies is broken. **G** Close to integer multiples of the EOD frequency of the receiver (here 800 Hz), slow amplitude modulations reoccur despite the high difference frequencies.

Grewe, and Benda, 2018). *Apteronotus leptorhynchus* habituates to specific beat frequencies (Harvey-Girard, Tweedle, Ironstone et al., 2010). Because beat frequency is a relative measure of EOD frequency of another fish it is not an unambiguous cue for species recognition. A negative difference frequency indicates a female for a high frequency *Apteronotus leptorhynchus* male, but can be an *Eigenmannia* for a low frequency male (Henninger, Krahe, Sinz, and Benda, 2020). In P-type electroreceptors, locking of action potentials to the absolute EOD frequency of the other fish could potentially disambiguate species recognition (Sinz, Sachgau, Henninger, Benda, and Grewe, 2020).

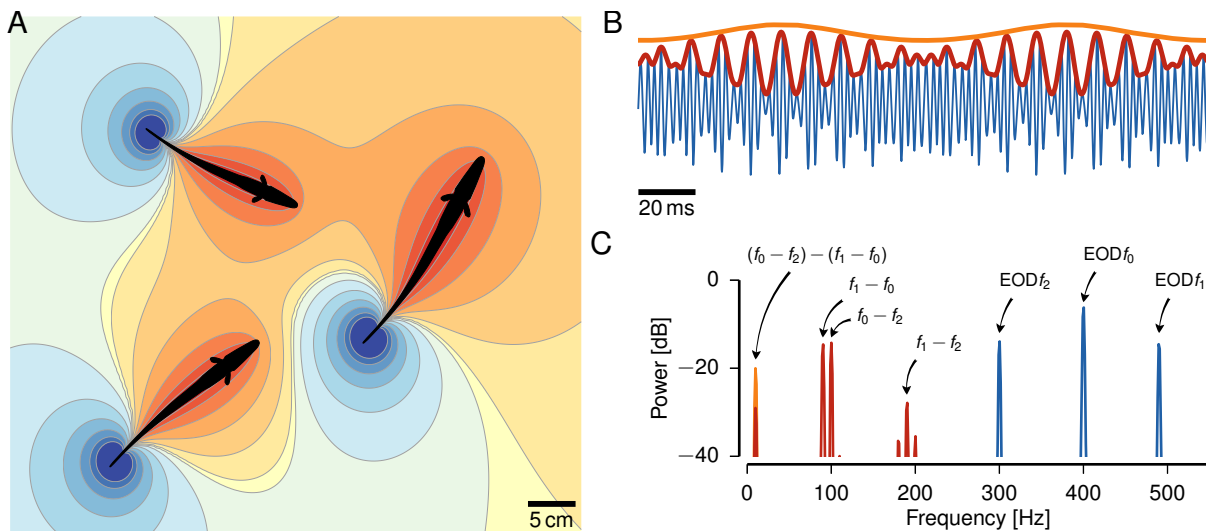


**Figure 19.9:** Multiple beats. **A** Three interacting wave-type electric fish. **B** Amplitude modulations more complex than beats result from such interactions with modulations on various time scales: a fast beat (red) and a slower envelope (orange). **C** In the power spectrum of the original modulated EOD of the receiver (blue) three peaks indicate the EOD frequencies of the three interacting fish (here at  $f_0 = 400$ ,  $f_1 = 490$  and  $f_2 = 300$  Hz). The power spectrum of the analytic signal displays the frequency components of the amplitude modulation (red). There are peaks at the pairwise difference frequencies (red). The low frequency peak at  $(f_0 - f_2) - (f_1 - f_0)$  makes up the slow envelope (orange), which is not a second order amplitude modulation.

### Beat waveform

For sinusoidal EOD waveforms negative and positive difference frequencies result in the same amplitude modulation (Fig. 19.8 E). This symmetry, however, is broken with more complex EOD waveforms (Fig. 19.8 F). Note that for small beat contrasts the waveform of the beat reflects the EOD waveform of the other fish (Petzold, Marsat, and Smith, 2016). The peaks of each EOD cycle of the receiver sample the EOD waveform of the other fish in a stroboscopic way (like the scanning behavior suggested for pulse fish by Hopkins, 1986). Whether fish use this information for species and/or sex identification is still debated (Kramer and Otto, 1988; Dunlap and Larkins-Ford, 2003; Fugère and Krahe, 2010). Difference frequencies approaching twice the EOD frequency of the receiving fish, again result in slow amplitude modulations (Fig. 19.8 G). Although behaviorally relevant for conspecific (Henninger, Krahe, Kirschbaum, Grewe, and Benda, 2018) and allospecific (Henninger, Krahe, Sinz, and Benda, 2020) communication, this regime is completely unexplored.

### Beat phases

Beat amplitude and beat frequency are fundamental signal parameter for P-type electroreceptor afferents. In addition to the amplitude modulation, beats also induce a phase modulation. An EOD of higher frequency than the receiver (positive difference frequency) results in slight phase delays during the falling flanks of the beating amplitude modulation, and in phase advances during the raising flanks. For negative difference frequencies (EOD frequency of the other fish is lower than the one of the receiving fish) this is reversed. By means of T-type electroreceptor afferents, electric fish can measure these phase modulations and compare them to the amplitude modulations in order to disambiguate the sign of difference frequencies. Beats do not generate any low-frequency signals relevant for the ampullary electrosensory system, because they are simply the sum of two fast mean-free oscillations.

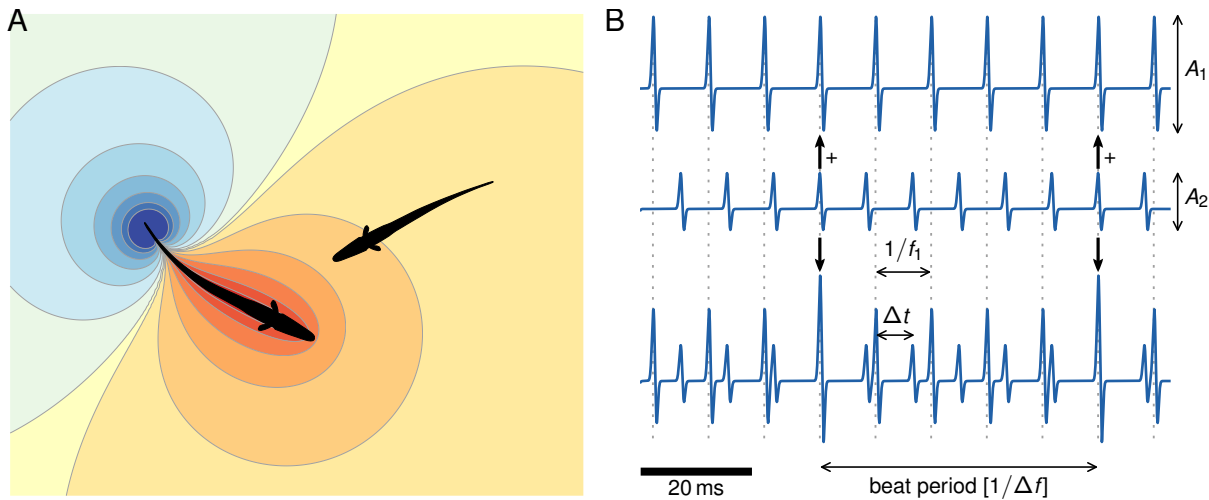


**Figure 19.10:** Beats of pulse-type electric fish. **A** Usually when one pulse-type fish is discharging the other one is silent — the electric fields of pulse-type electric fish do not interact. **B** EODs of two Gymnotiform pulse fish emitted periodically with two different EOD frequencies  $f_1$  and  $f_2$  (top and center). The phase  $\varphi = 2\pi\Delta t f_1$ , i.e. the distance  $\Delta t$  of the other fish's EODs from the previous one of the receiving fish relative to the period  $1/f_1$ , periodically decreases within each beat period. It can happen, that once in every beat cycle the two fish simultaneously emit an EOD, which then superimpose (vertical arrows).

### Multiple beats

In natural habitats often more than two fish are close to each other, both in social fish like *Eigenmannia* and more territorial *Apteronotus* (see for example Fig. 19.15, Stamper, Carrera-G, Tan et al., 2010; Henninger, Krahe, Sinz, and Benda, 2020). In spacious tanks in the laboratory, *Apteronotus leptorhynchus* also cluster at superior resting sites (Raab, Linhart, Wurm, and Benda, 2019).

Superpositions of EODs of more than two wave fish result in more complex amplitude modulations (Fig. 19.9, Middleton, Longtin, Benda, and Maler, 2006; Stamper, Carrera-G, Tan et al., 2010). These are superpositions of beats with all pairwise difference frequencies, differences of difference frequencies, and higher interactions between the involved EOD frequencies. Depending on the EOD frequencies and their relative amplitudes the power spectrum of the amplitude modulation can be more complex with many more peaks than the example shown. In the example the amplitude of a fast beat carrier is modulated by a slow envelope like signal corresponding to the lowest difference of difference frequencies (orange). Note that the corresponding low frequency peak is often already present in the power spectrum of the amplitude modulation. It is therefore not strictly a second order amplitude modulation (see below). In *Eigenmannia* this slow component evokes a behavioral response based on the jamming avoidance response (Stamper, Madhav, Cowan, and Fortune, 2012).

### 19.5.2 Pulse fish beats and communication signals

In particular in gymnotiform pulse fish with their periodic discharges, beats also exist. However, because pulse fish EODs are much shorter compared to the intervals between two successive EODs, the EODs of two fish rarely superimpose in contrast to the continuous superposition of EODs in wave fish (Fig. 19.10 A). During the beat the relative time of the other fish's EOD within the period of the receiving fish's EODs periodically decreases for positive difference frequencies and increases for negative difference frequencies. Once within a beat period the EODs of the two fish could coincide and superimpose (Fig. 19.10 B).

However, pulse fish actively control the timing of their pulses. Gymnotiformes avoid coincident pulses by slight changes in the inter pulse intervals (Capurro, Reyes-Parada, Olazabal et al., 1997), or by keeping a fixed delay to the other fish's pulses, known as echo response (Westby, 1981). This behavior is discussed as a jamming avoidance response, because coincident pulses would jam electrolocation. Mormyridae also display echo responses at fixed

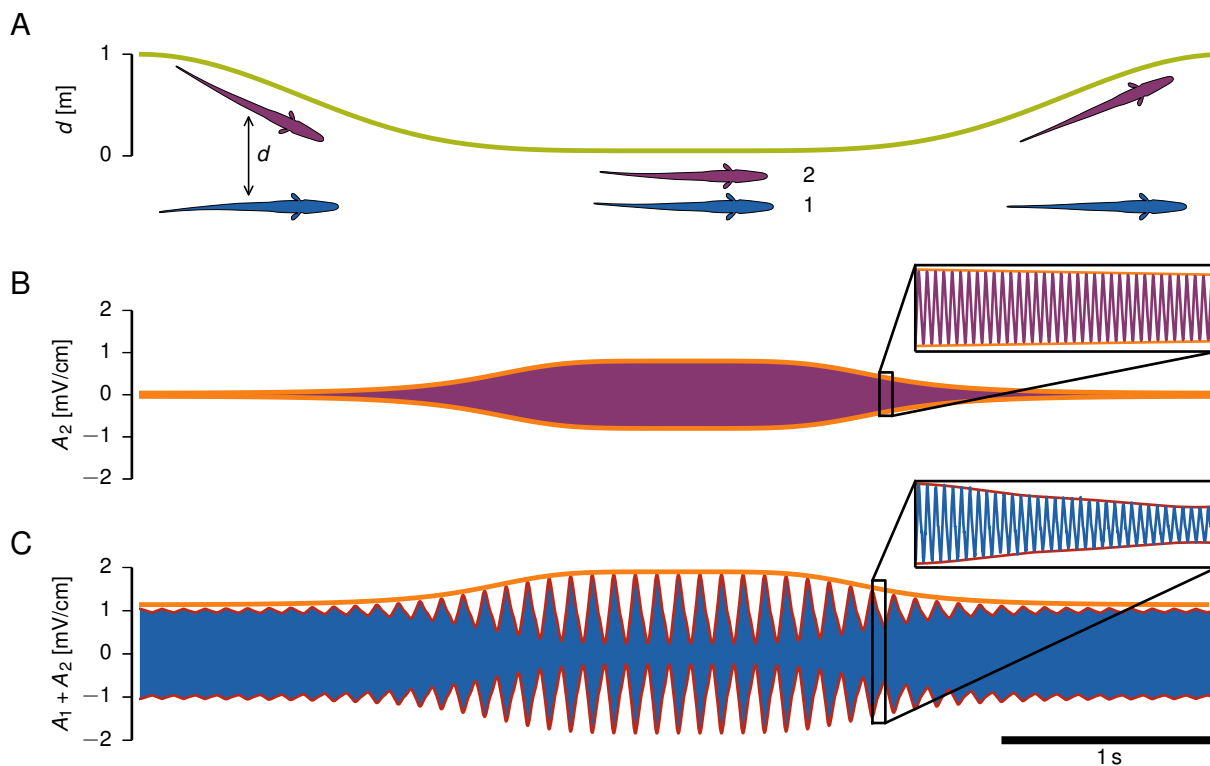


**Figure 19.11:** Motion envelopes. **A** The distance  $d$  between moving fish changes. **B** Consequently, the amplitude  $A_2$  of the other fish at the position of the receiving fish increases for decreasing distance and vice versa. **C** As a result, the beat at the receiving fish (red) changes its amplitude (orange), the motion envelope.

delays (Carlson, 2002) while foraging (Scheffell and Kramer, 2006) or as a pack cohesion signal (Arnégard and Carlson, 2005).

Common to both Gymnotiformes and Mormyridae pulse fish are various types of accelerations during which interpulse intervals are shortened. A prominent one is the novelty response, a sudden increase in discharge rate exponentially decaying back to baseline levels evoked by the detection of a novel object (Post and von der Emde, 1999). Many more types of accelerations are produced that differ in the duration, frequency excursion, and shape and are produced in different behavioral contexts like foraging, predation and agonistic encounters (Black-Cleworth, 1970; Carlson, 2002) and courtship (Wong and Hopkins, 2007). During cessations, emission of EODs is completely stopped for some time (Carlson, 2002; Silva, Quintana, Perrone, and Sierra, 2008). Bursts of very short interpulse intervals are accompanied by a reduction in EOD amplitude and have been observed in the context of courtship and breeding, both in Gymnotiformes (chirps, Silva, Quintana, Perrone, and Sierra, 2008) and Mormyridae (rasps, Hopkins and Bass, 1981).

### 19.5.3 Motion envelopes

Let's return to wave fish. The concept of a beat with a constant amplitude and frequency is an abstraction. Usually fish move relative to each other, come closer to each other or swim away from each other (Fig. 19.11 A). The amplitude of another fish at the position of a receiving fish is not constant; it depends on the distance between the two fish (Fig. 19.11 B). The amplitude is small for fish at larger distances and gets larger the closer the fish approach each other. Consequently, the beat amplitude is not constant, but changes according to these modulations of the other fish's amplitude (Fig. 19.11 C). This time dependent change of the beat amplitude caused by fish moving relative to each other is called the "motion envelope" (Yu, Hupé, Garfinkle, Lewis, and Longtin, 2005) or "movement envelope". Note that motion envelopes also result from turning fish because of the angular dependency



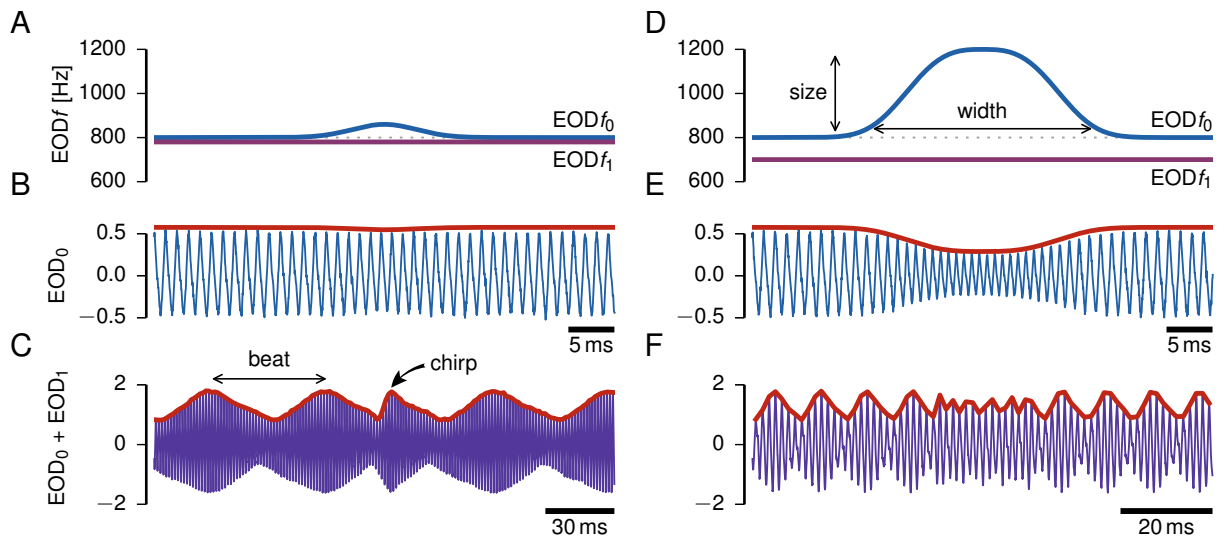


**Figure 19.12: Chirps.** **A** Chirps are transient increases in EOD frequency. During a small chirp of *Apteronotus leptorhynchus* (also known as type-2 chirp) EOD frequency is increased by  $\sim 60$  Hz during  $\sim 15$  ms (blue). **B** This brief frequency modulation is barely visible in the EOD of the fish emitting the chirp. The chirp is often accompanied by a small reduction in EOD amplitude (red). **C** Superimposed with the EOD of a receiving fish (purple), here with EOD frequency 20 Hz below the chirping fish (purple line in A), the small chirp has a marked effect on the amplitude modulation (red). The beat frequency is transiently increased by the chirp, resulting in about half a period of accelerated beat that induces a step-like increase in beat amplitude. **D** A large or type-1 chirp has a much larger increase in EOD frequency, the chirp size, of approximately  $\sim 400$  Hz. **E** In addition, the EOD amplitude (red) is reduced during the chirp. **F** As a result the beat amplitude is reduced during the chirp in addition to the accelerated beat.

of their dipolar electric field, Eq. (19.1).

The beat is a first order amplitude modulation of the EOD of the receiving fish. To extract the beat waveform from the EOD time course, a non-linear operation is required, e.g. magnitude of the analytic signal (Hilbert transform) or rectification with subsequent low-pass filtering (Stamper, Madhav, Cowan, and Fortune, 2012). Motion induced changes in the amplitude of the beat broaden the peak at the beat frequency in the power spectrum of the EOD's amplitude modulation. No peak at the motion's low frequency is created (Yu, Hupé, Garfinkle, Lewis, and Longtin, 2005). To extract this low frequency signal, a second nonlinear operation has to be applied on the beat waveform. This extracts the amplitude modulation of the amplitude modulation of the EOD carrier, the second order modulation. Second order modulations of the EOD are called “envelopes” in the electric fish literature (Middleton, Longtin, Benda, and Maler, 2006).

#### 19.5.4 Chirps

So far we discussed beats of two or more fish and motion envelopes arising from moving fish, all with the assumption that EOD frequencies are constant. However, electric fish modulate their EOD frequency on many different time scales ranging from few milliseconds to at least many minutes (Zakon, Oestreich, Tallarovic, and Triefenbach, 2002).

The fastest frequency modulation signals electric fish produce are so called “chirps”. During ten to a few hundred milliseconds EOD frequency is transiently increased by many ten up to several hundred Hertz (Fig. 19.12 A, D). Higher frequency excursions of the chirp are accompanied by amplitude reductions of the EOD (Fig. 19.12 B, E). Relevant for the receiving fish is the effect of a chirp on the amplitude modulation (Fig. 19.12 C, F). The increase in EOD frequency transiently changes the beat frequency. For small and short chirps on low beat frequencies this may apply to less than one beat period (Benda, Longtin, and Maler, 2005). An additional reduction in EOD amplitude during a chirp translates directly into a reduced beat amplitude during the chirp (Benda, Longtin, and Maler, 2006).



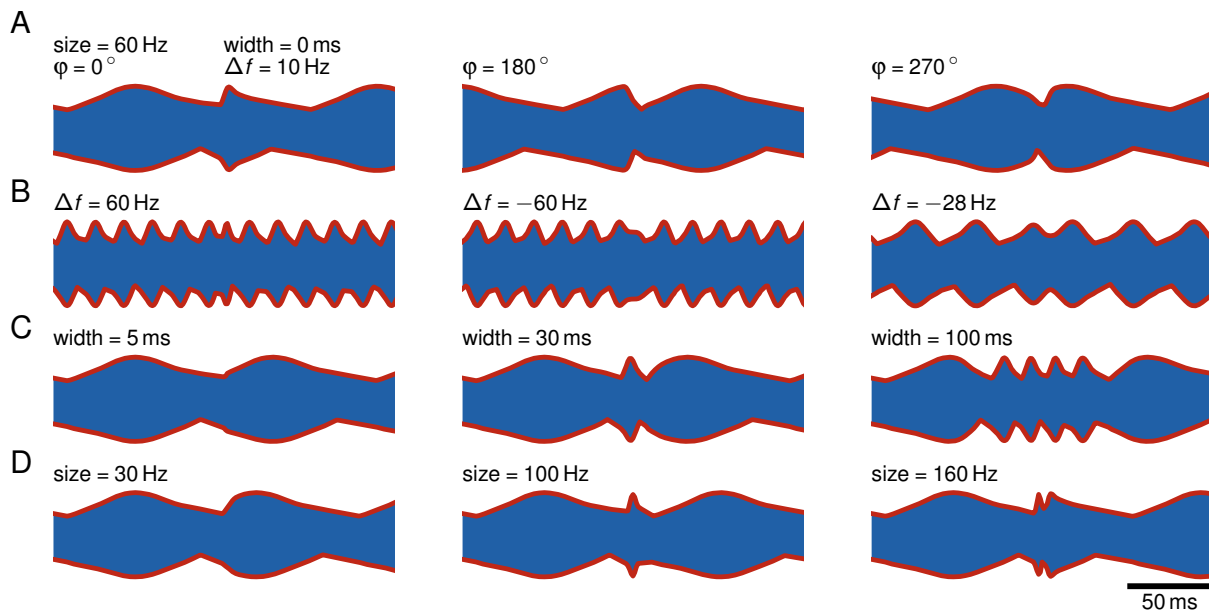


**Figure 19.13:** Amplitude modulations induced by chirps. Shown is a small chirp of *Apteronotus leptorhynchus* at the center of the beat waveforms. **A** Whether a small chirp induces an upstroke, a downstroke or something else in the amplitude modulation depends on the phase of the beat,  $\phi$ , at which the chirp occurs. **B** On positive difference frequencies,  $\Delta f$ , a chirp always accelerates the beat. On negative difference frequencies a chirp decelerates the beat. On small negative difference frequencies a chirp results in a transient phase reversal of the amplitude modulation. **C** The wider the chirp, the longer the time of accelerated beat cycles. **D** The larger the size of the chirp (its maximum increase in EOD frequency) the stronger the acceleration of the amplitude modulation.

Chirps thus introduce transient modulations of the ongoing periodic amplitude modulations of a beat. The resulting amplitude modulation evoked by a specific chirp depends on a number of factors. At low beat frequencies, the timing of the chirp within a beat period, the phase of the beat, strongly influences the resulting amplitude modulation (Fig. 19.13 A, Walz, Grewe, and Benda, 2014). It can vary from pure upstrokes to downstrokes. The difference frequency is the second, chirp independent factor (Fig. 19.13 B). On positive difference frequencies chirps transiently accelerate the beat, whereas on negative difference frequencies chirps decelerate the beat, slowing down the beat waveform. On small negative difference frequencies chirps introduce a transient phase reversal. Chirps thus disambiguate negative and positive difference frequencies (Walz, Grewe, and Benda, 2014). The longer the chirp the more beat cycles are accelerated by the chirp (Fig. 19.13 C). Chirp size, i.e. the frequency excursion of the chirp, affects the number and frequency of modified beat cycles (Fig. 19.13 D).

Chirps are very diverse and can be classified in a number of types that differ in chirp size, width and other features of their frequency modulation (Engler, Fogarty, Banks, and Zupanc, 2000). Chirp types are species specific (Turner, Derylo, de Santana, Alves-Gomes, and Smith, 2007; Petzold, Marsat, and Smith, 2016). *Eigenmannia* chirps are special in that they also generate a DC component that also excites the ampullary system (Stöckl, Sinz, Benda, and Grewe, 2014). Chirps play various roles in courtship and synchronization of spawning (Fig. 19.14, Hagedorn and Heiligenberg, 1985; Henninger, Krahe, Kirschbaum, Grewe, and Benda, 2018) and in aggression (Triefenbach and Zakon, 2008), most likely as submissive signals (Walz, Hupé, Benda, and Lewis, 2013; Henninger, Krahe, Kirschbaum, Grewe, and Benda, 2018). Chirp production recorded in artificial contexts in the lab are dramatically skewed towards aggressive behaviors compared to natural behaviors recorded in the wild (Henninger, Krahe, Kirschbaum, Grewe, and Benda, 2018). Echo responses in the range of 200 ms recorded in the wild (Henninger, Krahe, Kirschbaum, Grewe, and Benda, 2018) to a few seconds in the lab (Hupé and Lewis, 2008; Zupanc, Sîrbulescu, Nichols, and Ilies, 2006; Salgado and Zupanc, 2011) clearly qualify chirps as an electrocommunication signal.

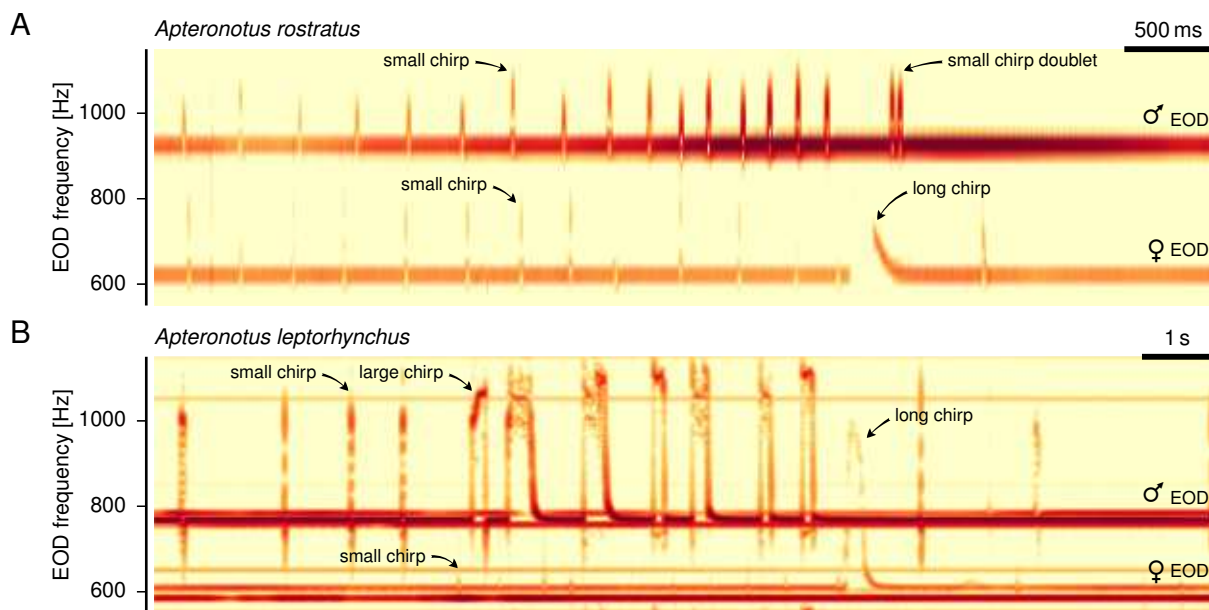


**Figure 19.14:** Chirps during courtship. **A** In *Apteronotus rostratus* recorded in Darien, Panamá, both male (top) and female (bottom) emit small chirps until the female emits a long chirp and the male acknowledges with a chirp doublet. **B** In *Apteronotus leptorhynchus* recorded in a tank in the lab males emit both small and large chirps when courting the female. The female responds with small chirps and eventually with a long chirp indicating the release of a single egg. Modified from Henninger, Krahe, Kirschbaum, Grewe, and Benda (2018).

### 19.5.5 Slow frequency modulations

In addition to chirps, wave-fish generate various types of frequency modulations on slower timescales, ranging from seconds to many minutes, with small frequency elevations of less than a few tens of Hertz (Fig. 19.15). Many of them resemble the different types of frequency accelerations reported from pulse fish (see above). Because these frequency modulations last much longer than typical beat periods, their effect is simply a prolonged frequency modulation of the beat, which most likely is accompanied by a motion envelope induced by the relative movement of the fish in these interactions.

Rises are characterized by a relatively fast onset within a few hundred milliseconds to a peak frequency, followed by an exponential decay back to baseline EOD frequency over many seconds (Hopkins, 1974a; Hagedorn and Heiligenberg, 1985). Rise durations cover a continuum ranging from less than a second (Fig. 19.15 Aa) to minutes (Fig. 19.15 Bb). The longer the rise, the higher its maximum frequency (Fig. 19.15 Aa,b, Engler, Fogarty, Banks, and Zupanc, 2000). Short rises are sometimes difficult to distinguish from small chirps (Kolodziejewski, Nelson, and Smith, 2005). Long rises can have a hump-like shape with a delayed peak, that sometimes is initiated by a transient frequency upstroke (Fig. 19.15 Cc, Zakon, Oestreich, Tallarovic, and Triefenbach, 2002). Although quite variable within a species, rises seem to be highly conserved between species (Turner, Derylo, de Santana, Alves-Gomes, and Smith, 2007). Rises are discussed as a signal in the context of aggression, appeasement and dominance (Hupé, Lewis, and Benda, 2008; Triefenbach and Zakon, 2008).

The jamming avoidance response (JAR) is a frequency modulation with an exponential onset with time constants in the range of seconds in response to another EOD with a frequency within  $\pm 20$  Hz (Bullock, Robert H. Hamstra, and Scheich, 1972; Dye, 1987). In *Eigenmannia* the JAR is an evasive frequency modulation that enlarges the difference frequency, probably in order to move the beat frequency outside the frequency range of electrolocation signals (Bullock, Robert H. Hamstra, and Scheich, 1972). In contrast, *Apteronotus leptorhynchus* only raises its frequency no matter whether the stimulating frequency was below or above the EOD frequency (Heiligenberg, Metzner, Wong, and Keller, 1996). In the lab, the typical JAR stimulus is an artificial EOD with constant amplitude and by some fixed frequency above or below the EOD frequency of the fish. Of course, the JAR

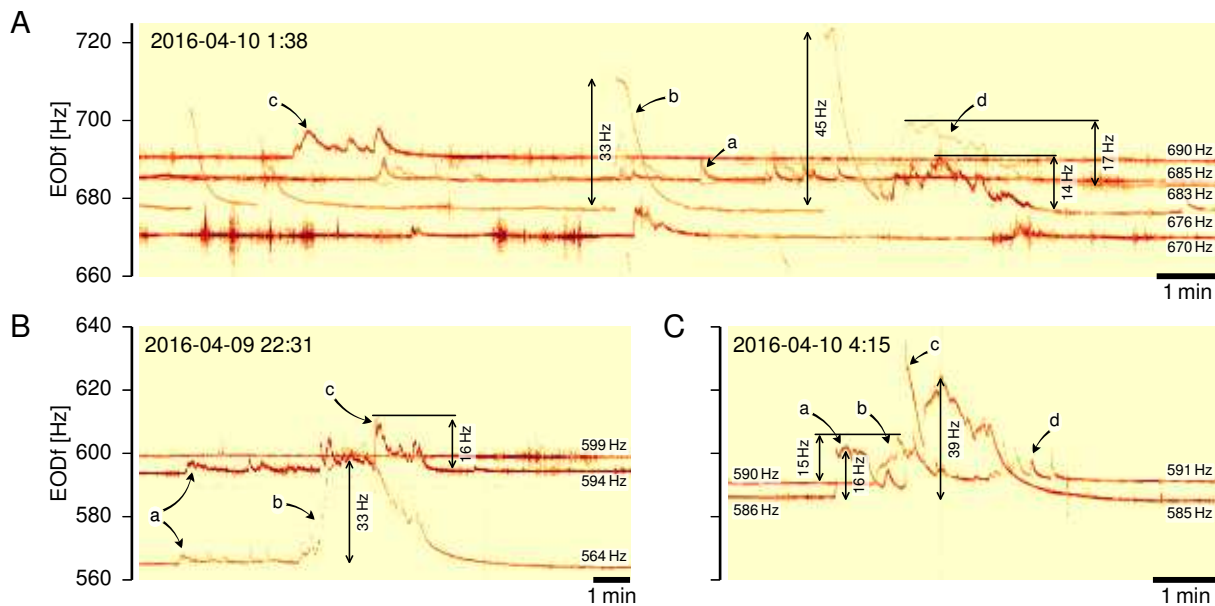


**Figure 19.15:** EOD frequency interactions in the wild. Spectrograms of *Aptereronotus macrostomus* recorded with an electrode array near San Martín, Meta region, Colombia, in April 2016 by Till Raab and Juan F. Sehuanes in collaboration with Jorge Molina. **A** Five fish separated by a few Hertz displaying a variety of small rises (a), large rises (b), multiple rises (c), and synchronous frequency increases (d). **B** The low frequency fish starts with a small frequency increase that is immediately mimicked by a fish with an 30 Hz higher EOD frequency (a). Then the low frequency fish rises its frequency slightly above the one of the other fish (b), which first slightly and then by 16 Hz evades this frequency attack (c). The third fish with the highest EOD frequency does not participate in this interaction. **C** A lower frequency fish overtakes the EOD frequency of another one considerably in two attempts, first by a small one (a) and then by a large and complex rise (marker c). The higher frequency fish responds with a much smaller increase in EOD frequency (b). After this interaction the two EOD frequencies are separated by additional 2 Hz compared to the situation before.

is also elicited by stimuli that are slowly faded in and out — stimuli that elicit motion envelopes.

Fish freely interacting in a larger tank (Tallarovic and Zakon, 2005) or in the wild (Fig. 19.15) show a wide range of frequency modulations. Some of them can be identified as rises, but JARs are much less obvious in such recordings. On the contrary, frequency interactions where fish approach (Fig. 19.15 A d) or even cross (Fig. 19.15 C) the EOD frequency of another fish are common. What these frequency battles mean and how they correlate with movements, dominance, and eventually reproductive success are wide open questions.

## 19.6 Conclusion — sensory ecology of electric fish

The electrosensory world of electric fish provides a diversity of natural and behaviorally relevant stimuli. Different qualities of these stimuli are sensed by three electrosensory pathways, the ampullary system for external low frequency signals, the amplitude and the time encoding pathways of the tuberous system for detecting modulations of the self-generated high-frequency electric field (see chapter Grewe). Together, these three electrosensory pathways make the electrosensory world colorful. Electric colors allow to infer electric material properties, in addition to detecting the mere presence of objects. In the case of electrolocating nearby objects, electric color is particularly useful in discriminating biotic from abiotic objects, and living from dead organisms. This is not so easily achieved with the lateral line system. Despite being limited to a small sensory volume around the fish (Snyder, Nelson, Burdick, and MacIver, 2007), this ability might be one of the subtle reasons why electric fish are so abundant in tropical freshwater habitats (Marrero and Taphorn, 1991; Cox-Fernandes, Podos, and Lundberg, 2004; Crampton, 2011).

In addition, electric fields of electric fish provide the possibility for communication over a few meter distance

(Knudsen, 1975; Henninger, Krahe, Kirschbaum, Grewe, and Benda, 2018). In contrast to auditory communication, the active electrosensory channel provides a relatively noise-free communication channel where abiotic noise sources are largely absent, but could be substantially cluttered by the presence of other electric fish (Hopkins, 1980; Henninger, Krahe, Sinz, and Benda, 2020).

As discussed in this chapter, we have a fairly good understanding of the physics and the basic concepts governing the electrosensory world. What we miss, however, is the sensory ecology of these fascinating fishes. We need more data on the electrical properties of prey, predators, plants, leaf litter, roots, logs, mud, sand and various types of rocks in the natural habitats of fish, together with prevalent water conductivities, to compare to EOD waveforms, frequencies and amplitudes in the context of specific foraging strategies, preferred prey, social life styles, predators, and microhabitat properties of the fish. We also need more data on the natural behaviors of electric fish to get better insights into their social lives, microhabitat use, movement patterns, etc. that all exert distinct selection pressures on the electrosensory system. With electrode arrays it is now possible to get detailed information on the secret lifestyles of electric fish even in their natural habitats (Henninger, Krahe, Kirschbaum, Grewe, and Benda, 2018; Henninger, Krahe, Sinz, and Benda, 2020; Madhav, Jayakumar, Demir et al., 2018).

Within the physical constraints of electrosensory worlds a number of selection pressures shape EOD waveforms, frequencies, and amplitudes. For example, EOD pulses of different mormyrid species are shorter the higher the density of fish, probably to reduce temporal overlap (Hopkins, 1980). Predators exert a selection pressure towards more symmetric and shorter EOD waveforms (Stoddard, Tran, and Krahe, 2019). There is a trend for EOD frequency to be higher in faster flowing waters (Crampton and Albert, 2006). In addition, sexual selection has a strong impact on EOD waveform diversity and speciation (Carlson, Hasan, Hollmann et al., 2011). These biotic factors seem to be the dominating factor shaping EOD waveforms (Crampton, Rodriguez-Cattáneo, Lovejoy, and Caputi, 2013). But how do these selection pressures interfere with the fish's ability to detect the electric color of their potential prey?

For bats we have a good understanding how the physics of the acoustic world shape adaptations to different foraging strategies in various habitats (Schnitzler and Kalko, 2001). Equivalently we need to understand the distinct electrical properties and challenges in the various ecological niches electric fish occupy. Fish hunting in open water face different problems than fish feeding on insect larvae sitting on substrates or buried in the mud. But it also makes a difference whether prey objects are sitting on plants or on rocks, because these substrates differ in their capacitive properties. Is there a species that specialized on terrestrial prey falling on the water surface (Winemiller and Adite, 1997)? Or is this a food source where the electric sense cannot compete with the lateral line? In contrast to bats, the communicative aspect of the electrosensory system is tightly interlinked with the localization aspect and has a strong influence on the evolution of EOD waveforms (Crampton, Rodriguez-Cattáneo, Lovejoy, and Caputi, 2013). To what extent can sexual selection push the parameters of electrosensory systems to the limits set by the physics of the ecological niche?

Electric fish live in an electric world. We need to put our electric goggles on to see how their environment and the way they use it looks like in its electrical properties. Only then can we understand the natural and sexual selection pressures acting on and shaping passive and active electrosensing in electric fish.

## 19.7 References

- Aguilera, P. A. and Caputi, A. A. (2003). Electoreception in *G. carapo*: detection of changes in waveform of the electrosensory signals. *J Exp Biol* **206**, 989–998.
- Ammari, H., Boulrier, T., Garnier, J., and Wang, H. (2014). Shape recognition and classification in electro-sensing. *PNAS* **111**, 11652–11657.
- Ammari, H., Boulrier, T., Garnier, J., and Wang, H. (2017). Mathematical modelling of the electric sense of fish: the role of multi-frequency measurements and movement. *Bioinspir Biomim* **12**, 025002.
- Arnegard, M. E. and Carlson, B. A. (2005). Electric organ discharge patterns during group hunting by a mormyrid fish. *Proc R Soc Lond B Biol Sci* **272**, 1305–1314.
- Arnegard, M. E., McIntyre, P. B., Harmon, L. J., Zelditch, M. L., Crampton, W. G. R., Davis, J. K., Sullivan, J. P.,

- Lavoué, S., and Hopkins, C. D. (2010). Sexual signal evolution outpaces ecological divergence during electric fish species radiation. *American Naturalist* **176**, 335–356.
- Assad, C., Rasnow, B., and Stoddard, P. K. (1999). Electric organ discharges and electric images during electrolocation. *J Exp Biol* **202**, 1185–1193.
- Babineau, D., Longtin, A., and Lewis, J. E. (2006). Modeling the electric field of weakly electric fish. *J Exp Biol* **209**, 3636–3651.
- Babineau, D., Longtin, A., and Lewis, J. E. (2007). Spatial acuity and prey detection in weakly electric fish. *PLoS Comput Biol* **3**, e38.
- Bacher, M. (1983). A new method for the simulation of electric fields, generated by electric fish, and their distortions by objects. *Biol Cybern* **47**, 51–58.
- Bastian, J. (1981). Electrolocation I. How electroreceptors of *Apteronotus albifrons* code for moving objects and other electrical stimuli. *J Comp Physiol A* **144**, 465–479.
- Belbenoit, P. (1970). Conditionnement instrumental de l'électroperception des objets chez *Gnathonemus petersii* (Mormyridae, Teleostei, Pisces). *Z vergl Physiol* **67**, 192–204.
- Bell, C. C., Bradbury, J., and Russell, C. J. (1976). The electric organ of a mormyrid as a current and voltage source. *J Comp Physiol* **110**, 65–88.
- Benda, J., Longtin, A., and Maler, L. (2005). Spike-frequency adaptation separates transient communication signals from background oscillations. *J Neurosci* **25**, 2312–2321.
- Benda, J., Longtin, A., and Maler, L. (2006). A synchronization-desynchronization code for natural communication signals. *Neuron* **52**, 347–358.
- Bennett, M. V. L. (1970). Comparative physiology: electric organs. *Annu Rev Physiol* **32**, 471–528.
- Bennett, M. V. L. (1971). Electroreception. *Fish Physiology* **5**, 493–574.
- Black-Cleworth, P. (1970). The role of electrical discharges in the non-reproductive social behaviour of *Gymnotus carapo* (Gymnotidae, Pisces). *Animal Behaviour Monographs* **3**, 1–78.
- Bleckmann, H. and Zelick, R. (2009). Lateral line system of fish. *Integrative Zoology* **4**, 13–25.
- Budelli, R. and Caputi, A. A. (2000). The electric image in weakly electric fish: perception of objects of complex impedance. *J Exp Biol* **203**, 481–492.
- Bullock, T. H. (1969). Species differences in effect of electroreceptor input on electric organ pacemakers and other aspects of behavior in electric fish. *Brain Behav Evol* **2**, 85–118.
- Bullock, T. H., Bodznick, D. A., and Northcutt, R. G. (1983). The phylogenetic distribution of electroreception: evidence for convergent evolution of a primitive vertebrate sense modality. *Brain Res Rev* **6**, 25–46.
- Bullock, T. H., Robert H. Hamstra, J., and Scheich, H. (1972). The jamming avoidance response of high frequency electric fish I. general features. *J Comp Physiol* **77**, 1–22.
- Burham, E. G., Huckaby, W. B., Gowdy, R., and Burns, B. (1969). Microvolt electric signals from fishes and the environment. *Science* **164**, 965–968.
- Capurro, A., Reyes-Parada, M., Olazabal, D., Perrone, R., Silveira, R., and Macadar, O. (1997). Aggressive behavior and jamming avoidance response in the weakly electric fish *Gymnotus carapo*: effects of 3,4-Methylenedioxymethamphetamine (MDMA). *Comp Biochem Physiol* **188A**, 831–840.
- Caputi, A. A. (1999). The electric organ discharge of pulse gymnotiforms: the transformation of a simple impulse into a complex spatiotemporal electromotor pattern. *J Exp Biol* **202**, 1229–1241.
- Caputi, A. A., Budelli, R., Grant, K., and Bell, C. C. (2000). The electric image in weakly electric fish: physical images of resistive objects in *Gnathonemus petersii*. *J Exp Biol* **203**, 481–492.
- Caputi, A. A., Castelló, M. E., Aguilera, P. A., Pereira, C., Nogueira, J., Rodríguez-Cattaneo, A., and Lezcano, C. (2008). Active electroreception in *Gymnotus omari*: imaging, object discrimination, and early processing of actively generated signals. *J Physiol Paris* **102**, 256–271.
- Caputi, A. A., Silva, A. C., and Macadar, O. (1998). The electric organ discharge of *Brachyhypopomus pinnicaudatus*. the effects of environmental variables on waveform generation. *Brain Behav Evol* **52**, 148–158.
- Carlson, B. A. (2002). Electric signaling behavior and the mechanisms of electric organ discharge production in mormyrid fish. *J Physiol Paris* **96**, 405–419.
- Carlson, B. A., Hasan, S. M., Hollmann, M., Miller, D. B., Harmon, L. J., and Arnegard, M. E. (2011). Brain



- evolution triggers increased diversification of electric fishes. *Science* **332**, 583–586.
- Castelló, M. E., Aguilera, P. A., Trujillo-Cenóz, O., and Caputi, A. A. (2000). Electoreception in *Gymnotus carapo*: pre-receptor processing and the distribution of electoreceptor types. *J Exp Biol* **203**, 3279–3287.
- Chen, L., House, J. L., Krahe, R., and Nelson, M. E. (2005). Modeling signal and background components of electrosensory scenes. *J Comp Physiol A* **191**, 331–345.
- Coates, C. W. (1954). Activity in electrogenic organs of knifefishes. *Science* **120**, 845–846.
- Cox-Fernandes, C., Podos, J., and Lundberg, J. G. (2004). Amazonian ecology: tributaries enhance the diversity of electric fishes. *Science* **305**, 1960–1962.
- Crampton, W. G. R. (2011). An ecological perspective on diversity and distributions. In Albert, J. S. and Reis, R. (eds.) *Historical biogeography of neotropical freshwater fishes*. University of California Press, California, pp. 165–189.
- Crampton, W. G. R. and Albert, J. S. (2006). Evolution of electric signal diversity in gymnotiform fishes. I. Phylogenetic systematics, ecology and biogeography. In Ladich, F., Collin, S. P., Moller, P., and Kapoor, B. G. (eds.) *Communication in fishes*. Science Publishers, Enfield, N.H., pp. 647–696.
- Crampton, W., Rodriguez-Cattáneo, A., Lovejoy, N., and Caputi, A. (2013). Proximate and ultimate causes of signal diversity in the electric fish gymnotus. *J Exp Biol* **216**, 2523–2541.
- Dunlap, K. D. and Larkins-Ford, J. (2003). Diversity in the structure of electrocommunication signals within a genus of electric fish, *Apteronotus*. *J Comp Physiol A* **189**, 153–161.
- Dunlap, K. D. and Oliveri, L. M. (2002). Retreat site selection and social organization in captive electric fish, *Apteronotus leptorhynchus*. *J Comp Physiol A* **188**, 469–477.
- Dunlap, K. D., Smith, G. T., and Yekta, A. (2000). Temperature dependence of electrocommunication signals and their underlying neural rhythms in the weakly electric fish, *Apteronotus leptorhynchus*. *Brain Behav Evol* **55**, 152–162.
- Dunlap, K., Thomas, P., and Zakon, H. (1998). Diversity of sexual dimorphism in electrocommunication signals and its androgen regulation in a genus of electric fish, *Apteronotus*. *J Comp Physiol A* **183**, 77–86.
- Dye, J. (1987). Dynamics and stimulus-dependence of pacemaker control during behavioral modulations in the weakly electric fish, *Apteronotus*. *J Comp Physiol A* **161**, 175–185.
- von der Emde, G. (1990). Discrimination of objects through electrolocation in the weakly electric fish, *Gnathonemus petersii*. *J Comp Physiol A* **167**, 413–421.
- von der Emde, G. (1993). The sensing of electrical capacitances by weakly electric mormyrid fish: effects of water conductivity. *J Exp Biol* **181**, 157–173.
- von der Emde, G. (1998). Capacitance detection in the wave-type electric fish *Eigenmannia* during active electrolocation. *J Comp Physiol A* **182**, 217–224.
- von der Emde, G. and Ringer, T. (1992). Electrolocation of capacitive objects in four species of pulse-type weakly electric fish. *Ethology* **91**, 326–338.
- von der Emde, G. and Ronacher, B. (1994). Perception of electric properties of objects in electrolocating weakly electric fish: two-dimensional similarity scaling reveals a City-Block metric. *J Comp Physiol A* **175**, 801–812.
- von der Emde, G., Schwarz, S., Gomez, L., Budelli, R., and Grant, K. (1998). Electric fish measure distance in the dark. *Nature* **395**, 890–894.
- Enger, P. S. and Szabo, T. (1968). Effect of temperature on the discharge rates of the electric organ of some gymnotids. *Comp Biochem Physiol* **27**, 625–627.
- Engler, G., Fogarty, C., Banks, J., and Zupanc, G. (2000). Spontaneous modulations of the electric organ discharge in the weakly electric fish, *apteronotus leptorhynchus*: a biophysical and behavioral analysis. *J Comp Physiol A* **186**, 645–660.
- Escamilla-Pinilla, C., Mojica, J. I., and Molina, J. (2019). Spatial and temporal distribution of *Gymnorhamphichthys rondoni* (Gymnotiformes: Rhamphichthyidae) in a long-term study of an amazonian terra firme stream, Leticia - Colombia. *Neotropical Ichthyology* **17**, e190006.
- Fechler, K. and von der Emde, G. (2013). Figureground separation during active electrolocation in the weakly electric fish, *Gnathonemus petersii*. *J Physiol Paris* **107**, 72–83.
- Feulner, P. G. D., Plath, M., Engelmann, J., Kirschbaum, F., and Tiedemann, R. (2009). Electrifying love: electric-



- fish use species-specific discharge waveform recognition. *Biol Lett* **5**, 225–228.
- Fotowat, H., Harrison, R., and Krahe, R. (2013). Statistics of the electrosensory input in the freely swimming weakly electric fish *Apteronotus leptorhynchus*. *J Neurosci* **33**, 13758–13772.
- Franchina, C. R. and Stoddard, P. K. (1998). Plasticity of the electric organ discharge waveform of the electric fish *Brachyhypopomus pinnicaudatus* I. quantification of day-night changes. *J Comp Physiol A* **183**, 759–768.
- Friedman, M. A. and Hopkins, C. D. (1996). Tracking individual mormyrid electric fish in the field using electric organ discharge waveforms. *Anim Behav* **51**, 391–407.
- Fugère, V. and Krahe, R. (2010). Electric signals and species recognition in the wave-type gymnotiform fish *Apteronotus leptorhynchus*. *J Exp Biol* **213**, 225–236.
- Fugère, V., Ortega, H., and Krahe, R. (2011). Electrical signalling of dominance in a wild population of electric fish. *Biol Lett* **7**, 197–200.
- Fujita, K. and Kashimori, Y. (2010). Modeling the electric image produced by objects with complex impedance in weakly electric fish. *Biol Cybern* **103**, 105–118.
- Fujita, K. and Kashimori, Y. (2019). Representation of objects shape by multiple electric images in electrolocation. *Biol Cybern* **113**, 239–255.
- Gavassa, S., Silva, A. C., Gonzalez, E., and Stoddard, P. K. (2012). Signal modulation as a mechanism for handicap disposal. *Anim Behav* **83**, 935–944.
- Gottwald, M., Bott, R. A., and von der Emde, G. (2017). Estimation of distance and electric impedance of capacitive objects in the weakly electric fish *Gnathonemus petersii*. *J Exp Biol* **220**, 3142–3153.
- Gottwald, M., Singh, N., Haubrich, A., Regett, S., and von der Emde, G. (2018). Electric-color sensing in weakly electric fish suggests color perception as a sensory concept beyond vision. *Curr Biol* **220**, 3142–3153.
- Graff, C. and Kramer, B. (1992). Trained weakly-electric fishes *Pollimyrus isidori* and *Gnathonemus petersii* (Mormyridae, Teleostei) discriminate between waveforms of electric pulse discharges. *Ethology* **90**, 279–292.
- Hagedorn, M. (1988). Ecology and behavior of a pulse-type electric fish, *Hypopomus occidentalis* (Gymnotiformes, Hypopomidae), in a fresh-water stream in Panama. *Copeia* **1988**, 324–335.
- Hagedorn, M. and Heiligenberg, W. (1985). Court and spark: electric signals in the courtship and mating of gymnotoid fish. *Anim Behav* **33**, 254 – 265.
- Hagiwara, S. and Morita, H. (1963). Coding mechanisms of electroreceptor fibers in some electric fish. *J Neurophysiol* **26**, 551–567.
- Harder, W., Schief, A., and Uhlemann, H. (1964). Zur Funktion des Elektrischen Organs von *Gnathonemus petersii* (Gthr. 1862) (Mormyriiformes, Teleostei). *Zeitschrift für vergleichende Physiologie* **48**, 302–331.
- Harvey-Girard, E., Tweedle, J., Ironstone, J., Cuddy, M., Ellis, W., and Maler, L. (2010). Long-term recognition memory of individual conspecifics is associated with telencephalic expression of Egr-1 in the electric fish *Apteronotus leptorhynchus*. *J Comp Neurol* **518**, 2666–2692.
- Heiligenberg, W. (1973). Electrolocation of objects in the electric fish *Eigenmannia* (Rhamphichthyidae, Gymnotoidei). *J Comp Physiol* **87**, 137–164.
- Heiligenberg, W. (1975). Theoretical and experimental approaches to spatial aspects of electrolocation. *J Comp Physiol* **103**, 247–272.
- Heiligenberg, W. and Altes, R. A. (1978). Phase sensitivity in electroreception. *Science* **199**, 1001–1003.
- Heiligenberg, W., Metzner, W., Wong, C. J. H., and Keller, C. H. (1996). Motor control of the jamming avoidance response of *Apteronotus leptorhynchus*: evolutionary changes of a behavior and its neuronal substrates. *J Comp Physiol A* **179**, 653–674.
- Henninger, J., Krahe, R., Kirschbaum, F., Grewe, J., and Benda, J. (2018). Statistics of natural communication signals observed in the wild identify important yet neglected stimulus regimes in weakly electric fish. *J. Neurosci.* **38**, 5456–5465.
- Henninger, J., Krahe, R., Sinz, F., and Benda, J. (2020). Tracking activity patterns of a multispecies community of gymnotiform weakly electric fish in their neotropical habitat without tagging. *J Exp Biol* **223**, jeb206342.
- Hofmann, V., Sanguinetti-Scheck, J. I., Gómez-Sena, L., and Engelmann, J. (2013). From static electric images to electric flow: Towards dynamic perceptual cues in active electroreception. *J Physiol Paris* **107**, 95–106.
- Hofmann, V., Sanguinetti-Scheck, J. I., Gómez-Sena, L., and Engelmann, J. (2017). Flow as a basis for a novel

- distance cue in freely behaving electric fish. *J Neurosci* **37**, 302–312.
- Hopkins, C. D. (1972). Sex differences in electric signaling in an electric fish. *Science* **176**, 1035–1037.
- Hopkins, C. D. (1974a). Electric communication: functions in the social behavior of *Eigenmannia virescens*. *Behavior* **50**, 270–304.
- Hopkins, C. D. (1974b). Electric communication in the reproductive behavior of *Sternopygus macrurus* (gymnotoidei). *Z Naturf* **35**, 518–535.
- Hopkins, C. D. (1980). Evolution of electric communication channels of mormyrids. *Behav Ecol Sociobiol* **7**, 1–13.
- Hopkins, C. D. (1986). Temporal structure of non-propagated electric communication signals. *Brain Behav Evol* **28**, 43–59.
- Hopkins, C. D. (1999). Design features for electric communication. *J Exp Biol* **202**, 1217–128.
- Hopkins, C. D. and Bass, A. H. (1981). Temporal coding of species recognition signals in an electric fish. *Science* **212**, 85–87.
- Hopkins, C. D., Comfort, N. C., Bastian, J., and Bass, A. H. (1990). Functional analysis of sexual dimorphism in an electric fish, *Hypopomus pinnicaudatus*, order Gymnotiformes. *Brain Behav Evol* **35**, 350–367.
- Hopkins, C. D. and Heiligenberg, W. F. (1978). Evolutionary designs for electric signals and electroreceptors in gymnotoid fishes of Surinam. *Behav Ecol Sociobiol* **3**, 113–134.
- Hopkins, C. D. and Westby, G. W. M. (1986). Time domain processing of electric organ discharge waveforms by pulse-type electric fish. *Brain Behav Evol* **29**, 77–104.
- Hoshimiya, N., Shogen, K., Matsuo, T., and Chichibu, S. (1980). The *Apteronotus* EOD field: waveform and EOD field simulation. *J Comp Physiol* **135**, 283–290.
- Hupé, G. and Lewis, J. (2008). Electrocommunication signals in free swimming brown ghost knifefish, *apteronotus leptorhynchus*. *J Exp Biol* **211**, 1657–67.
- Hupé, G. J., Lewis, J. E., and Benda, J. (2008). The effect of difference frequency on electrocommunication: chirp production and encoding in a species of weakly electric fish, *Apteronotus leptorhynchus*. *J Physiol Paris* **102**, 164–172.
- Jun, J. J., Longtin, A., and Maler, L. (2014). Enhanced sensory sampling precedes self-initiated locomotion in an electric fish. *J Exp Biol* **217**, 3615–3628.
- Kalmijn, A. J. (1974). The detection of electric fields from inanimate and animate sources other than electric organs. In Fessard, A. (ed.) *Electroreceptors and other specialized receptors in lower vertebrates*. Springer, Heidelberg, pp. 148–194.
- Kirschbaum, F. (1983). Myogenic electric organ precedes the neurogenic organ in apteronotid fish. *Naturwissenschaften* **70**, 205–207.
- Knudsen, E. (1975). Spatial aspects of the electric fields generated by weakly electric fish. *J Comp Physiol A* **99**, 103–118.
- Kolodziejewski, J. A., Nelson, B. S., and Smith, G. T. (2005). Sex and species differences in neuromodulatory input to a premotor nucleus: a comparative study of substance P and communication behavior in weakly electric fish. *J Neuro Biol* **62**, 299–315.
- Kramer, B. (1999). Waveform discrimination, phase sensitivity and jamming avoidance in a wave-type electric fish. *J Exp Biol* **202**, 1387–1398.
- Kramer, B., Kirschbaum, F., and Markl, H. (1981). Species specificity of electric organ discharges in a sympatric group of gymnotoid fish from Manaus (Amazonas). *Adv Physiol Sci* **31**, 195–219.
- Kramer, B. and Otto, B. (1988). Female discharges are more electrifying: spontaneous preference in the electric fish, *Eigenmannia* (Gymnotiformes, Teleostei). *Behav Ecol Sociobiol* **23**, 55–60.
- Lissmann, H. W. (1951). Continuous electrical signals from the tail of a fish, *Gymnarchus niloticus* cuvier. *Nature* **167**, 201–202.
- Lissmann, H. W. (1958). On the function and evolution of electric organs in fish. *J Exp Biol* **35**, 156–191.
- Lissmann, H. W. and Machin, K. E. (1958). The mechanism of object location in *Gymnarchus niloticus* and similar fish. *J Exp Biol* **35**, 451–486.
- Lissmann, H. W. and Schwassmann, H. O. (1965). Activity rhythm of an electric fish, *Gymnorhamphichthys hypostictus*.

- tomus, ellis. *Z vergl Physiol* **51**, 153–171.
- Machnik, P. and Kramer, B. (2008). Female choice by electric pulse duration: attractiveness of the males' communication signal assessed by female bulldog fish, *Marcusenius pongolensis* (Mormyridae, Teleostei). *J Exp Biol* **211**, 1969–1977.
- MacIver, M. A., Patankar, N. A., and Shirdgaonkar, A. A. (2010). Energy-information trade-offs between movement and sensing. *PLoS Comput Biol* **6**, e1000769.
- Madhav, M. S., Jayakumar, R. P., Demir, A., Stamper, S. A., Fortune, E. S., and Cowan, N. J. (2018). High-resolution behavioral mapping of electric fishes in amazonian habitats. *Scientific Reports* **8**.
- Marrero, C. and Taphorn, D. C. (1991). Notas sobre la historia natural y la distribucion de los peces Gymnotiformes em la cuenca del Rio Apure y otros rios de la Orinoquia. *Biollania* **8**, 123–142.
- McKibben, J. R., Hopkins, C. D., and Yager, D. D. (1993). Directional sensitivity of tuberous electroreceptors: polarity preferences and frequency tuning. *J Comp Physiol A* **173**, 415–424.
- Meyer, J. H. (1982). Behavioral responses of weakly electric fish to complex impedances. *J Comp Physiol* **145**, 459–470.
- Meyer, J. H., Leong, M., and Keller, C. H. (1987). Hormone-induced and maturational changes in electric organ discharges and electroreceptor tuning in the weakly electric fishapteronotus. *J Comp Physiol A* **160**, 385–394.
- Middleton, J. W., Longtin, A., Benda, J., and Maler, L. (2006). The cellular basis for parallel neural transmission of a high-frequency stimulus and its low-frequency envelope. *PNAS* **103**, 14596–14601.
- Migliaro, A., Caputi, A. A., and Budelli, R. (2005). Theoretical analysis of pre-receptor image conditioning in weakly electric fish. *PLoS Comput Biol* **1**, e16.
- Moortgat, K., Keller, C., Bullock, T., and Sejnowski, T. (1998). Submicrosecond pacemaker precision is behaviorally modulated: the gymnotiform electromotor pathway. *PNAS* **95**, 4684–4689.
- Nelson, M. E. and MacIver, M. A. (1999). Prey capture in the weakly electric fish apteronotus albifrons: sensory acquisition strategies and electrosensory consequences. *J Exp Biol* **202**, 1195–1203.
- Nelson, M. E. and MacIver, M. A. (2006). Sensory acquisition in active sensing systems. *J Comp Physiol A* **192**, 573–586.
- Pedraja, F., Aguilera, P., Caputi, A. A., and Budelli, R. (2014). Electric imaging through evolution, a modeling study of commonalities and differences. *PLoS Comput Biol* **10**, e1003722.
- Pedraja, F., Hofmann, V., Lucas, K. M., Young, C., Engelmann, J., and Lewis, J. E. (2018). Motion parallax in electric sensing. *PNAS* **115**, 573–577.
- Pereira, A. C., Aguilera, P., and Caputi, A. A. (2012). The active electrosensory range of *Gymnotus omarorum*. *J Exp Biol* **215**, 3266–3280.
- Peters, R. C. and Bretschneider, F. (1972). Electric phenomena in the habitat of the catfish *Ictalurus nebulosus* LeS. *J Comp Physiol* **81**, 345–362.
- Petzold, J. M., Marsat, G., and Smith, G. T. (2016). Co-adaptation of electric organ discharges and chirps in South American ghost knifefishes (Apteronotidae). *J Physiol Paris* **110**, 200–215.
- Post, N. and von der Emde, G. (1999). The "novelty response" in an electric fish: response properties and habituation. *Physiol Behav* **68**, 115–128.
- Pusch, R., von der Emde, G., Hollmann, M., Bacelo, J., Nöbel, S., Grant, K., and Engelmann, J. (2008). Active sensing in a mormyrid fish: electric images and peripheral modifications of the signal carrier give evidence of dual foveation. *J Exp Biol* **211**, 921–9334.
- Raab, T., Linhart, L., Wurm, A., and Benda, J. (2019). Dominance in habitat preference and diurnal explorative behavior of the weakly electric fish apteronotus leptorhynchus. *Frontiers in Integrative Neuroscience* **13**, 21.
- Rasnow, B. and Bower, J. M. (1996). The electric organ discharges of the gymnotiform fishes: I. *Apteronotus leptorhynchus*. *J Comp Physiol A* **178**, 383–396.
- Rodríguez-Cattáneo1, A., Aguilera, P., Cilleruelo, E., Crampton, W. G. R., and Caputi1, A. A. (2013). Electric organ discharge diversity in the genus *Gymnotus*: anatomo-functional groups and electrogenic mechanisms. *J Exp Biol* **216**, 1501–1515.
- Roth, A. (1972). Wozu dienen die Elektrozeporen der Welse? *J Comp Physiol* **79**, 113–135.
- Salgado, J. A. G. and Zupanc, G. K. (2011). Echo response to chirping in the weakly electric brown ghost knifefish

- (*Apteronotus leptorhynchus*): role of frequency and amplitude modulations. *J Can Zool* **89**, 498–508.
- Sanguinetti-Scheck, J. I., Pedraja, E. F., Cilleruelo, E., Migliaro, A., Aguilera, P., Caputi, A. A., and Budelli, R. (2011). Fish geometry and electric organ discharge determine functional organization of the electrosensory epithelium. *PLoS ONE* **6**, e27470.
- de Santana, C. D., Crampton, W. G. R., Dillman, C. B., Frederico, R. G., Sabaj, M. H., Covain, R., Ready, J., Zuanon, J., de Oliveira, R. R., Mendes-Júnior, R. N., Bastos, D. A., Teixeira, T. F., Mol, J., Ohara, W., e Castro, N. C., Peixoto, L. A., Nagamachi, C., Sousa, L., Montag, L. F. A., Ribeiro, F., Waddell, J. C., Piorsky, N. M., Vari, R. P., and Wosiacki, W. B. (2019). Unexpected species diversity in electric eels with a description of the strongest living bioelectricity generator. *Nat Commun* **10**, 4000.
- Scheffel, A. and Kramer, B. (2006). Intra- and interspecific electrocommunication among sympatric mormyrids in the upper Zambezi river. In Ladich, F., Collin, S. P., Moller, P., and Kapoor, B. G. (eds.) *Communication in fishes*. Science Publishers, Enfield, N.H., pp. 733–751.
- Schnitzler, H.-U. and Kalko, E. K. V. (2001). Echolocation by insect-eating bats. *BioScience* **51**, 557–569.
- Schwan, H. P. (1963). Electric characteristic of tissues. *Biophysik* **1**, 198–208.
- Schwarz, S. and von der Emde, G. (2001). Distance discrimination during active electrolocation in the weakly electric fish *Gnathonemus petersii*. *J Comp Physiol A* **186**, 1185–1197.
- Sicardi, E. A., Caputi, A. A., and Budelli, R. (2000). Physical basis of distance discrimination in weakly electric fish. *Physica A* **283**, 86–93.
- Silva, A., Perrone, R., and Macadar, O. (2007). Environmental, seasonal, and social modulations of basal activity in a weakly electric fish. *Physiol Behav* **90**, 525–536.
- Silva, A., Quintana, L., Galeano, M., Errandonea, P., and Macadar, O. (1999). Water temperature sensitivity of EOD waveform in *Brachyhypopomus pinnicaudatus*. *J Comp Physiol A* **185**, 187–197.
- Silva, A., Quintana, L., Perrone, R., and Sierra, F. (2008). Sexual and seasonal plasticity in the emission of social electric signals. behavioral approach and neural bases. *J Physiol Paris* **102**, 272–278.
- Sim, M. and Kim, D. (2011). Electrolocation based on tail-bending movements in weakly electric fish. *J Exp Biol* **214**, 2443–2450.
- Sinz, F. H., Sachgau, C., Henninger, J., Benda, J., and Grewe, J. (2020). Simultaneous spike-time locking to multiple frequencies. *J Neurophysiol* **123**, 2355–2372.
- Smith, G. T. (2013). Evolution and hormonal regulation of sex differences in the electrocommunication behavior of ghost knifefishes (apteronotidae). *J Exp Biol* **216**, 2421–2433.
- Snyder, J. B., Nelson, M. E., Burdick, J. W., and MacIver, M. A. (2007). Omnidirectional sensory and motor volumes in electric fish. *PLoS Biol* **5**, e301.
- Squire, A. and Moller, P. (1982). Effects of water conductivity on electrocommunication in the weak-electric fish *Brienomyrus niger* (Mormyriiformes). *Anim Behav* **30**, 375–382.
- Stamper, S. A., Carrera-G, E., Tan, E. W., Fugère, V., Krahe, R., and Fortune, E. S. (2010). Species differences in group size and electrosensory interference in weakly electric fishes: Implications for electrosensory processing. *Behav Brain Res* **207**, 368 – 376.
- Stamper, S. A., Madhav, M. S., Cowan, N. J., and Fortune, E. S. (2012). Beyond the Jamming Avoidance Response: weakly electric fish respond to the envelope of social electrosensory signals. *J Exp Biol* **215**, 4196–4207.
- Steinbach, A. B. (1970). Diurnal movements and discharge characteristics of electric gymnotid fishes in the Rio Negro, Brazil. *Biol Bull* **138**, 200–210.
- Stöckl, A., Sinz, F., Benda, J., and Grewe, J. (2014). Encoding of social signals in all three electrosensory pathways of *Eigenmannia virescens*. *J Neurophysiol* **112**, 2076–2091.
- Stoddard, P. K. (1999). Predation enhances complexity in the evolution of electric fish signals. *Nature* **400**, 254–256.
- Stoddard, P. K. and Markham, M. R. (2008). Signal cloaking by electric fish. *BioScience* **58**, 415–425.
- Stoddard, P. K., Rasnow, B., and Assad, C. (1999). Electric organ discharges of the gymnotiform fishes: III. *Brachyhypopomus*. *J Comp Physiol A* **184**, 609–630.
- Stoddard, P. K., Tran, A., and Krahe, R. (2019). Predation and crypsis in the evolution of electric signaling in weakly electric fishes. *Front Ecol Evol* **7**, 264.

- Tallarovic, S. K. and Zakon, H. H. (2005). Electric organ discharge frequency jamming during social interactions in brown ghost knifefish, *apteronotus leptorhynchus*. *Anim Behav* **70**, 1355 – 1365.
- Triefenbach, F. and Zakon, H. (2008). Changes in signalling during agonistic interactions between male weakly electric knifefish, *Apteronotus leptorhynchus*. *Anim Behav* **75**, 1263–1272.
- Turner, C. R., Derylo, M., de Santana, C. D., Alves-Gomes, J. A., and Smith, G. T. (2007). Phylogenetic comparative analysis of electric communication signals in ghost knifefishes (Gymnotiformes: Apteronotidae). *J Exp Biol* **210**, 4104–4122.
- Walz, H., Grewe, J., and Benda, J. (2014). Static frequency tuning accounts for changes in neural synchrony evoked by transient communication signals. *J Neurophysiol* **112**, 752–765.
- Walz, H., Hupé, G. J., Benda, J., and Lewis, J. E. (2013). The neuroethology of electrocommunication: How signal background influences sensory encoding and behaviour in *Apteronotus leptorhynchus*. *J Physiol Paris* **107**, 13–25.
- Westby, G. W. M. (1981). Communication and jamming avoidance in electric fish. *Trends Neurosci* **4**, 205–210.
- Westby, G. W. M. and Kirschbaum, F. (1981). Sex differences in the electric organ discharge of *Eigenmannia virescens* and the effect of gonadal maturation. *Adv Physiol Sci* **31**, 179–194.
- Winemiller, K. O. and Adite, A. (1997). Convergent evolution of weakly electric fishes from floodplain habitats in Africa and South America. *Environmental Biology of Fishes* **49**, 175–186.
- Wong, R. Y. and Hopkins, C. D. (2007). Electrical and behavioral courtship displays in the mormyrid fish *Brienomyrus brachyistius*. *J Exp Biol* **210**, 2244–2525.
- Yu, N., Hupé, G., Garfinkle, C., Lewis, J. E., and Longtin, A. (2005). Coding conspecific identity and motion in the electric sense. *PLoS Comput Biol* **8**, e1002564.
- Zakon, H. H., Oestreich, J., Tallarovic, S., and Triefenbach, F. (2002). EOD modulations of brown ghost electric fish: JARs, chirps, rises, and dips. *J Physiol Paris* **96**, 451–458.
- Zupanc, G. K. H., Sîrbulescu, R. F., Nichols, A., and Ilies, I. (2006). Electric interactions through chirping behavior in the weakly electric fish, *Apteronotus leptorhynchus*. *J Comp Physiol A* **192**, 159–173.